Early life nociception is influenced by peripheral growth hormone signaling

Adam J. Dourson[1], Zachary K. Ford[1], Kathryn J. Green[1], Carolyn E. McCrossan[1], Megan C. Hofmann[1], Renita C. Hudgins[1], Michael P. Jankowski[1,2,3*]

[1] Department of Anesthesia, [2] Center for Understanding Pediatric Pain, Cincinnati Children's Hospital Medical Center, [3] Department of Pediatrics, University of Cincinnati, College of Medicine, Cincinnati, OH 45229

***Corresponding author:**

Michael P. Jankowski

3333 Burnet Avenue, MLC6016

Cincinnati, Ohio 45229-3026

Telephone: (513) 803-7966

E-mail: michael.jankowski@cchmc.org

Conflict of interest:

The authors declare no competing financial interests.

Abstract

A number of cellular systems work in concert to modulate nociceptive processing in the periphery, but the mechanisms that regulate neonatal nociception may be distinct compared to adults. Our previous work indicated a relationship between neonatal hypersensitivity and growth hormone (GH) signaling. Here, we explored the peripheral mechanisms by which GH modulated neonatal nociception under normal and injury conditions (incision). We found that GH receptor signaling in primary afferents maintains a tonic inhibition of peripheral hypersensitivity. After injury, a macrophage dependent displacement of injury-site GH was found to modulate neuronal transcription at least in part via serum response factor regulation. A single GH injection into the injured hindpaw muscle effectively restored available GH signaling to neurons and prevented acute pain-like behaviors, primary afferent sensitization, and neuronal gene expression changes. GH treatment also inhibited long-term somatosensory changes observed after repeated peripheral insult. Results may indicate a novel mechanism of neonatal nociception.

Introduction

Functional restoration after tissue injury requires a coordinated response between immune cells, neurons, and local tissues within the affected area. This response further generates a nociceptive signal via primary sensory neurons that is required to inform the organism of the ongoing repair process (Baoge et al., 2012) (Sass et al., 2018) (McMahon et al., 2015) (Basbaum et al., 2009) (Philippou et al., 2012). Responses from each of these individual cell types play a role in how a noxious signal is transduced into the central nervous system (CNS) e.g. (Basbaum et al., 2009).

The immature dorsal root ganglion (DRG) contains a compilation of functional sensory neuron subtypes that is distinct from adults (Jankowski et al., 2014) (Sharma et al., 2020). As such, neonates are particularly vulnerable to sensory impairment during developmental injury (Lim and Godambe, 2017). Recent work in animals (Ren et al., 2004) (Walker et al., 2009) and humans (Hermann et al., 2006) (Walker et al., 2018) (Moriarty et al., 2018) (Walker, 2019) indicates that early life injury enhances pain-related responses later in life. These “priming” effects of neonatal injury have been linked to alterations in the central nervous system (Walker et al., 2016) (Baccei, 2016) (Brewer and Baccei, 2019). However, evidence suggests that there is also a peripheral component that has been less explored (Moriarty et al., 2018). We have shown that the pattern of primary afferent sensitization and injury-related receptor/channel expression in the DRGs after neonatal peripheral injury is unique to that observed in adult nociceptors (Jankowski et al., 2014) (Liu et al., 2017) (Ye and Woodbury, 2010) (Koerber et al., 2010) (Koerber and Woodbury, 2002). Altogether, this suggests that the mechanisms of nociception in neonates may be somewhat distinct.

We recently found that growth hormone (GH) may be one factor involved in generalized pain-related responses to peripheral injury in neonates (Liu et al., 2017) (Ford et al., 2019). The

pituitary gland generates GH, which is crucial for normal growth and development. The largest increases in systemic GH levels are known to occur during early postnatal development, which corresponds with the most rapid growth period (Bartholomew EF, 2009). This is the same developmental period when GH was found to substantially influence pain-like responses and primary afferent function (Liu et al., 2017) (Ford et al., 2019). Specifically, inflammatory nociception was correlated with a reduction of site-specific cutaneous GH levels that could be prevented by systemic GH treatment. These effects may have been due to direct GH modulation of receptor/channel expression in neonatal DRGs (Liu et al., 2017) (Ford et al., 2019).

GH receptors (GHr) typically affect cellular functions through activation of various transcription factors such as the signal transducers and activators of transcription (STATs), serum response factor (SRF) or ERK like kinases (ELKs) (Ceseña et al., 2007). These factors can also be invoked in response to an aversive peripheral stimulus and can modulate both transcriptional and behavioral phenotypes (Salaffi et al., 2018) (Gomez et al., 2018). Immune cells that infiltrate injury sites release a variety of cytokines and growth factors during repair that can themselves be pro-nociceptive (Ren and Dubner, 2010) (McMahon et al., 2005) (McMahon et al., 2015) (Basbaum et al., 2009) (Philippou et al., 2012). Interestingly, macrophages in particular are known to use peripheral GH to modulate local inflammation (Govers et al., 1999) (Strous et al., 1996) (Lu et al., 2013) (Schneider et al., 2019). Taken together, altered GH signaling within primary afferent neurons may regulate receptor expression to modulate peripheral sensitization and subsequent pain-like behaviors in coordination with the infiltrating immune cells (Basbaum et al., 2009) (McMahon et al., 2015) (Ford et al., 2019).

In support of this, clinical reports show that in addition to growth problems, many children with GH deficiency (Pinho-Ribeiro et al., 2018) (Cuatrecasas, 2009) (Dattani and Preece, 2004)

report pain (Cimaz et al., 2001). Other studies have found that exogenous GH treatment may be an effective pain therapy for patients with erythromelalgia (Cimaz et al., 2001), fibromyalgia (Cuatrecasas et al., 2014) (Cuatrecasas et al., 2010) (Cuatrecasas et al., 2012) (Cuatrecasas et al., 2007) or low back pain (Dubick et al., 2015). Conversely, GH receptor blockers, used to treat acromegaly, can produce pain [e.g.] (van der Lely et al., 2001). Thus, understanding the mechanisms of how GH regulates pain-like responses may help us understand basic nociceptive processing in the immature nervous system. Here, we explored how GH modulated nociception under normal and injury-related (incision) conditions in neonatal mice. We tested the hypothesis that GH modulates pain-related behaviors and primary afferent sensitization after neonatal muscle incision through unique endocrine-peripheral nervous-and immune system interactions.

Results

Sensory neuron specific deletion of growth hormone receptor modulates peripheral responsiveness in uninjured neonatal mice.

Previously, we have demonstrated that a systemic reduction in growth hormone levels resulted in neonatal hypersensitivity (postnatal day 7 (P7)-P14) to peripheral stimuli that resolved by P21 (Ford et al., 2019). To determine if the effects of reduced GH-signaling on nociception were peripherally mediated, we injected growth hormone binding protein (GHBP) locally into the right hind paw of uninjured neonatal (P7-P14) mice. We found that one day after injection, GHBP resulted in spontaneous paw guarding behaviors (Fig. 1a). To then test if the anti-nociceptive effects of GH were due to a direct effect on primary afferents, we developed a transgenic mouse that allowed for targeted deletion of GHr in a time dependent manner in sensory neurons. We crossed the advillin (Adv)-creERT2 mouse (Lau et al., 2011) with a floxed GHr line and injected neonatal pups with tamoxifen at P7 to initiate sensory neuron specific deletion of GHr (Fig. 1b). Using this strategy, we first confirmed that control animals expressed normal levels of GHr in the DRGs while tamoxifen injected Adv;GHr$^{f/f}$ neonates had significantly reduced GHr expression as assessed with immunocytochemistry (Fig. 1b',b''). Realtime PCR analysis confirmed that within 5-7 days post tamoxifen injection, that GHr mRNA was significantly reduced in the DRGs compared to controls (-45 ± 25% vs. controls; n=5-13 per group; $p<0.05$). This corresponded with an upregulation of insulin-like growth factor receptor 1 (IGFr1) (136 ± 46% vs. control; $p<0.05$) as well as serum response factor (SRF) mRNA (229 ± 52% vs. control; $p<0.05$) confirming previous literature (Carter-Su et al., 2016) that these factors are downstream of growth hormone signaling. Interestingly, STAT5 was not altered in the DRGs of tamoxifen injected Adv;GHr$^{f/f}$ mice (7 ± 41% vs. control; $p>0.05$). We then performed behavioral analyses in these animals and found that although proprioception (righting reflexes) was unaffected by the sensory neuron targeted knockout of GHr (Fig. 1c), we detected alterations in other behaviors. Static cutaneous mechanical responsiveness (von Frey filament withdrawal

thresholds), and withdrawal thresholds to probing of the muscles (muscle squeezing) were significantly altered by GHr knockout in uninjured animals (Fig. 1d,e). Further, in a dynamic neonatal muscle strength assay, we again found that, unlike littermate controls, animals with sensory neuron specific GHr knockout did not significantly increase in strength over time (Fig. 1f). Area under the curve (AUC) analysis indicates that neonates with GHr mutations have lower overall cutaneous and muscle withdrawal thresholds and muscle strength scores compared to control animals (Fig. 1d',e',f').

Local injection of GH at the time of neonatal muscle incision blocks behavioral hypersensitivity and primary afferent sensitization.

Since peripheral GH signaling to neurons appeared to significantly influence nociception during early postnatal development, we wanted to test whether this pathway could also modulate injury-related hypersensitivity in the periphery. In order to assess this, we utilized a "reverse" hindpaw incision model in which surgical incision of the flexor digitorum brevis (FDB) muscles was obtained from the dorsal side of the foot through the hairy skin. The rationale for performing incision in this manner was to reduce cutaneous injury site effects when assessing muscle-specific pain-related behaviors (muscle squeezing). The surgical model produces robust pain-related hypersensitivity in neonates and also allowed us to deliver GH directly to the injury site. In these assays, we used an outbred mouse line to increase generalizability of the potential effects. We first confirmed that a neonatal "reverse" muscle incision resulted in detectable pain-like phenotypes, while an incision only of the hairy skin did not (Suppl. Fig. 1) similar to previous work (Brennan et al., 1996) (Baccei, 2016). We therefore assessed the levels of GH in the muscle after incision using western blot (Fig. 2a) and found that one day after surgery, muscle GH levels were significantly reduced. This corresponded with the observed spontaneous paw guarding behaviors and muscle mechanical hypersensitivity induced by incision one day later (Fig. 2b,c). To determine if local injection of GH could blunt incision-related hypersensitivity, we

first performed a dose response analysis (Suppl. Fig. 1) based on doses of GH that were insufficient to alter functional levels of systemic insulin-like growth factor 1 (IGF-1) (Farris et al., 2007). We confirmed that a single injection of GH (1.5mg/kg in 10µL) into the incision site was able to restore muscle GH levels similar to naïve mice (Fig. 2a). Importantly, we then found that paw guarding scores and muscle mechanical withdrawal thresholds were normalized to baseline (BL) levels by this single injection of GH into the incision site compared to vehicle injected neonates with incision (Fig. 2b,c). By three days following the surgical incision, we no longer detected hypersensitivity in vehicle injected controls or GH treated animals (Fig. 2b,c). Interestingly, delayed GH treatment partially blocked spontaneous paw guarding if given within 8 hours (Fig. 2d) of surgery, possibly indicating a time sensitive application window. The local injection of GH at this dose was not sufficient to alter the cross-sectional area of individual muscle fibers or change physiological conditions of the animals including body temperature and weight. GH injection into uninjured animals also had no effects on baseline animal behaviors (Suppl. Fig. 2). We then wanted to determine if the anti-nociceptive effects of GH treatment could be observed in older animals, but found that adolescent animals (P35) do not display altered muscle growth hormone levels after an injury. Further, these animals do not show any alterations in pain-related behaviors after muscle incision in response to local GH treatment at this dose (Suppl. Fig. 1). These data suggest that GH can modulate pain-like behaviors specifically in neonates.

Next, we used a novel neonatal *ex vivo* electrophysiological single unit recording preparation (Fig. 2e) to assess the response properties of individual primary muscle afferents in mice with incision. We found that the distribution of functional primary muscle afferents was altered by incision. Fewer mechanically sensitive group III and group IV muscle afferents (14/50, 28%) were observed in mice with muscle incision plus vehicle injection compared to naïve. A similar reduction in the numbers of innocuous metabolite (“low” responders) responsive units was also

observed (2/13, 15%) that corresponded with an increase in the numbers of chemically sensitive cells that responded to both innocuous and noxious ("high" responders) metabolite mixtures (7/13, 54%). Local GH injection completely reversed the incision-related effects on muscle afferent prevalence (Fig. 2f). We also found that mechanically sensitive muscle sensory neurons had lower thresholds to mechanical deformation of the muscle receptive fields after incision plus vehicle injection, but animals treated with GH at the time of the incision did not differ in mechanical thresholds compared to naïve (Fig. 2g). GH treated animals also showed decreased firing rates (FRs) to mechanical stimuli compared to mice with incision although neither group differed from naïve (Fig. 2h,i). The firing rates of thermally and chemically activated cells were not altered. The mean peak instantaneous frequencies were not statistically altered under any condition in any group (Suppl. Table 1). Taken together, exogenous local growth hormone treatment can prevent pain-related behaviors and primary afferent sensitization observed in neonates with muscle incision.

Incision-induced transcriptional changes in the DRG can be blocked by GH treatment. To determine potential underlying neuronal mechanisms by which growth hormone mediated anti-nociception after neonatal muscle incision, we analyzed mRNA levels in the DRGs for genes previously found to be altered during neonatal injury (Jankowski et al., 2014) among others known to regulate sensory responsiveness in the periphery in animals one day after injury (see full list in Table 1). Similar to that observed in mice with sensory neuron specific knockout of the GHr (see above), we found that muscle incision induced a significant increase in IGFr1 mRNA in the DRGs. Also upregulated was the proton sensor and heat transducing channel, TRPV1 and the environmental irritant and cold receptor, TRPA1. ATP sensing ion channel, P2X3 and the proton responsive channel, ASIC3, for example were not altered by incision. Interestingly, GH treatment at the time of injury blocked the upregulation of all of these factors (Table 1).

To assess if GH could also modulate injury related changes in gene expression in the injured muscles, we then analyzed the expression of candidate cytokines and growth factors known to be altered after injury in the periphery. Muscle incision significantly upregulated monocyte chemoattractant protein 1 (MCP-1), glial cell line-derived neurotrophic factor (GDNF), interleukin 1β (IL1β), and nerve growth factor (NGF), but not tumor necrosis factor alpha (TNFα). Interestingly, none of these factors were altered by local GH treatment (Table 1). Together, data suggests that GH provides a tonic control of gene expression in the DRG, but exogenous GH treatment at low doses may not alter the inflammatory response to incision within the muscles.

SRF upregulation in the DRGs modulates pain-related behaviors following surgical incision.

To begin to understand the mechanism by which GHr signaling effected neonatal nociception, we screened a number of known downstream transcription factors in the DRGs (Table 1). Neonates with muscle incision plus vehicle injection displayed significant upregulation of SRF, STAT3 and 5, and a significant downregulation of ERK like kinase 3 (ELK3), but no changes in ELK 1 or ELK4. Injection of GH into the muscles after incision specifically blocked the injury-related upregulation of SRF and STAT5. Since genetic knockout of GHr in uninjured sensory neurons regulated SRF expression (above) and to determine the role that one of these factors may play in muscle incision-induced hypersensitivity in neonates, we utilized our *in vivo* nerve-targeted siRNA knockdown strategy to inhibit the DRG upregulation of SRF (Jankowski et al., 2009) (Liu et al., 2017). Prior to incision, animals were injected with Penetratin-linked siRNAs against SRF (PenSRF) into the right sciatic nerve. We found that this strategy partially, but significantly blunted the upregulation of SRF in the DRGs at the mRNA and protein levels (Fig. 3a,b). We then assessed incision-related hypersensitivity in animals with the targeted knock down of SRF and found that inhibition of this transcription factor significantly reduced spontaneous paw guarding compared to neonates with control siRNA injection (PenCON) plus

incision (Fig. 3c). Additionally, incision-related muscle mechanical hypersensitivity observed in mice with PenCON injection was also inhibited in mice with SRF knockdown (Fig. 3d). Interestingly, while PenSRF inhibited both guarding and mechanical hypersensitivity in males, female guarding was unaffected by PenSRF injection (Suppl. Fig 3). These behavioral changes corresponded with inhibition of TRPA1 upregulation after SRF knockdown DRGs (PenCON = 493 ± 41%*, $p<0.05$, PenSRF = 52 ± 37%, $p>0.05$; vs. naïve, n = 3-6/group). Interestingly, TRPV1 upregulation was not altered (PenCON = 90 ± 16%*, PenSRF = 128 ± 13%*, $p<0.05$ vs. naïve, n = 3-6/group). Together, these data indicate one neuronal transcriptional pathway downstream of GHr that may modulate neonatal nociception.

GH sequestering by infiltrating macrophages regulates incision-related hypersensitivity in neonates.

In our current and previous reports (Liu et al., 2017), we have shown that the levels of GH decrease in the injured tissue within one day. However, the mechanism behind this reduction in GH levels were previously unknown. Using immunohistochemical analyses, we observed that GH is normally found in a diffuse pattern between myofibers within the muscles of naïve neonates (Fig. 4a). However, after incision, we found that GH was displaced in the muscle tissue into a more concentrated, localized manner (Fig. 4b). The areas of intense GH staining appeared to be monocyte-like based on qualitative morphological assessments. We therefore used a transgenic mouse line in which a tdTomato reporter was expressed in monocytes and mature macrophages (LysM-Cre;td-Tom) and performed immunohistochemistry for GH in these mice with incision. While non-incised hind paws have few detectable macrophages within the muscles (Suppl. Fig. 4), animals that received a muscle incision have abundant numbers of macrophages at the injury site. Further, the concentrated pattern of GH staining in mice with incision was found to overlap significantly with the tdTomato reporter (Fig. 4c,d), while this is not observed in uninjured tissue (Suppl. Fig. 4). Previous work has suggested that macrophages

can bind and internalize GH (Govers et al., 1999) (Strous et al., 1996) (Lu et al., 2013). Since tissue collection for our western blot analyses was obtained from animals with cardiac perfusion and samples for IHC were obtained from snap-frozen, fresh tissues (un-perfused), we posited that the “reduction” in muscle GH levels observed after incision were due to macrophage dependent sequestering. We found that following cardiac perfusion with ice cold saline in mice with incision, macrophages were no longer detected within the muscle. Moreover, in un-perfused neonates, there was no detectable reduction in GH using western blot analysis (Suppl. Fig. 4).

Data thus suggested that under neonatal injury conditions, infiltrating macrophages may sequester GH and thereby effectively remove the tonic signal that GH normally provides to innervating primary afferents. To test this hypothesis, we first treated incised animals intramuscularly with clodronate liposomes to deplete the infiltrating macrophages. Following surgery, this depletion prevented evoked muscle hypersensitivity but not spontaneous paw guarding behaviors (Suppl. Fig. 5). As macrophages appeared to at least play some role in incision-related hypersensitivity in neonates, we then analyzed incised animals with the GHr knocked out on macrophages and mature monocytes (LysM-Cre;GHr$^{f/f}$; MacGHr-/-). Since these animals are an inbred strain, we first confirmed that incision-related hypersensitivity was similar to that observed in the outbred Swiss Webster mice previously used in this report (Suppl. Fig. 5). Following this, we then found that animals with the GHr knocked out in macrophages still display infiltration of these immune cells within the muscles after incision, but they do not contain GH (Fig. 4e). We also found no reduction in muscle GH levels in these mice after injury and perfusion, unlike that observed in WT animals (Fig. 4e). The MacGHr-/- mice also displayed significantly less paw guarding (Fig. 4f) and did not exhibit reduced muscle withdrawal thresholds one day after injury (Fig. 4g) unlike control mice. Mechanical hypersensitivity from

the injury was not detected at 3d in either group, but unlike MacGHr-/- mice, controls still displayed a small guarding response at 3d (Suppl. Fig. 5).

We also analyzed the transcriptional changes within DRGs and the injured muscles from these mice. Receptors and channels shown previously (Table 1) to be upregulated in animals after injury were also observed in control mice with incision, but these same receptors were not upregulated in MacGHr-/- animals with incision (Fig. 4h). However, the upregulation of muscle cytokines and growth factors observed in control animals with incision were unaffected by knockout of GHr in macrophages. In fact, the levels of some of these factors were significantly greater in MacGHr-/- mice with incision compared to incised controls (Fig. 4i). These data indicate that macrophages may sequester muscle GH after injury, likely removing the tonic inhibition that GH provides on primary afferent neurons and leads to injury-induced pain-related behaviors.

Early life growth hormone reduction regulates neonatal "priming" of nociceptive responses to injury later in life.

To determine if GH-related anti-nociception could modulate the prolonged effects of repeated injury, we first assessed whether GH deficiency alone could induce a prolonged hypersensitivity after incision. In order to test this, we used the GH releasing hormone receptor (GHRHr) knockout mice that we have previously shown to display neonatal specific hypersensitivity (Ford et al., 2019) and performed a single incision in these mice at P35. At baseline (BL), we detected no difference between WT controls (GHRHr+/+), heterozygous GHRHr mutants (GHRHr+/-) and the homozygous GHRHr knockout (GHRHr-/-) mice. However, GHRHr-/- animals and to a degree, GHRHr+/- mice, displayed prolonged spontaneous paw guarding (Fig. 5a) and muscle withdrawal thresholds (Fig. 5b) after P35 incision compared to WT controls. We then confirmed previous reports (Walker et al., 2009) (Moriarty et al., 2018) that an early life muscle incision

(P7) in WT control mice followed by a P35 incision resulted in a longer lasting mechanical hypersensitivity compared to mice with P35 incision alone. Interestingly, if treatment with GH was given at the time of the early life injury (P7), prolonged hypersensitivity was not detected after the second incision (Fig. 5c). These data support our earlier findings that GHr signaling in early life is important for sensitization and disruptions in this signaling can induce long term somatosensory alterations in response to injury later in life.

Discussion

Our data indicate that in neonates, growth hormone expressed throughout the hindpaw muscles tonically activates the growth hormone receptor on neurons. This maintains basal transcription factor levels in sensory neurons, which supports normal afferent function. However, after an early life injury, macrophage infiltration results in an immune cell-dependent sequestration of muscle GH. The displacement of GH within the muscle removes GH signaling to neurons resulting, at least in part, in SRF-dependent transcription of sensory-related receptors/channels in the affected DRGs. Restoring the basal levels of GH (through targeted injections or by preventing the macrophage dependent sequestration), maintains neuronal GHr signaling and blocks peripheral sensitization (Fig. 6). GH signaling to immature neurons also appears to modulate injury responses later in life (Fig. 5). Thus, in neonates, a unique immune system dependent modulation of endocrine communication with the peripheral nervous system is accessed after injury to regulate nociception.

Nociception involves a variety of distinct extracellular and intracellular neuronal mechanisms, each of which can play a unique role in how peripheral stimuli are perceived upon transmission to the CNS (Julius and Basbaum, 2001). Throughout development distinct neurotrophic factors regulate neuronal subtype formation and innervation; however, these signaling growth factors also display non-canonical roles (Moqrich et al., 2004) (Shelton and Reichardt, 1984) (Mendell, 1996). Recent investigations also demonstrate that developing sensory neurons display changing transcriptional identities and functional maturation from the neonatal period through adulthood (Sharma et al., 2020) (Jankowski et al., 2014) (Adelman et al., 2019). While growth factors clearly alter subtype survival, we detect that modulation of neuronal GH signaling results in functional changes to normal somatosensory processing in both the skin (Ford et al., 2019) and the muscle. GH may have a more global effect on afferent function that influences somatosensory development unique to that observed with neurotrophic factors.

Recent data also suggests that the developmental stage of the animal may affect how primary afferents respond to injury (Jankowski et al., 2014). Further, the developing immune system shows unique characteristics resulting in a microenvironment that is distinct from that of older subjects (Kumar and Bhat, 2016) (Winterberg et al., 2015) (Weston et al., 1977). Here, we show that GH may have specific roles in regulating multiple cell types in the periphery after insult. Due to the unique developmental functions of primary afferents and the immune systems, neonatal injury may engage a distinct cellular interaction through which GH ultimately modulates neonatal nociception and injury-related hypersensitivity (Figs. 2-6). It is worth noting that the ages we detect GH-related effects on nociception are also when systemic GH is at its highest, and is critical for overall growth and development, which may account for its age-specific effects (Muller et al., 1999) (Figs. 1,2; Suppl. Figs. 1,2). Together, this evidence indicates a critical period in which the nervous, immune and endocrine systems uniquely interact to modulate peripheral sensitization.

Following a noxious stimulus, primary afferents respond by initiating various intracellular cascades that result in an upregulation of factors that change how the neuron responds to specific sensory stimuli (Basbaum et al., 2009). In our current work, we found that neonatal incision upregulated SRF and STAT5 in the DRGs, which could be blocked by intramuscular GH treatment (Fig. 2; Table 1). However, only SRF was found to be altered in the DRGs in our sensory neuron GHr knockout animal (Fig. 1). SRF is a well-studied transcription factor that operates in a complex within the nucleus to regulate gene expression in an age-controlled manner (Zhang et al., 2014). Further, SRF is a downstream target of canonical GH signaling (Carter-Su et al., 2016). We were able to show that incision-induced upregulation of SRF is important for at least TRPA1, but not TRPV1 upregulation after incision. STAT5 is another interesting target that is regulated by muscle GH signaling to neurons after injury, but not GHr

signaling directly. It is possible that STAT5 has the ability to transcriptionally control TRPV1 (TargetScanMouse and miRDB), but that upregulation of this transcription factor under neonatal injury conditions is due to non-GHr related signaling pathways such as neurotrophins or immune mediators (Gouin et al., 2017) (Kao et al., 2012). This will be an important area of future investigation.

The pathway by which growth hormone receptor targets these transcription factors is unknown. We are currently pursuing different mechanisms in which a loss of neuronal GHr signaling results in an increase of SRF dependent afferent sensitization. It is likely that a number of alterations are induced by both injury and GH signaling resulting in an intracellular dynamic that collectively modulates sensitization. Further analyses will be necessary to determine this.

Immune system regulation of the affected microenvironment is a well-known phenomenon following many different injury types (Basbaum et al., 2009) (Julius and Basbaum, 2001). The peripheral immune system reacts to an injury by mobilizing in stages with macrophages being one of the first responders (Fig. 4). This effect may be more heavily relied upon in neonates that have yet to fully develop; especially adaptive immune responses (Winterberg et al., 2015). We detected a time-dependent window for the local injection of GH that, if given 8 hours after the injury, only partially blocks sensitization (Fig. 2d). It may be that this time point corresponds with the infiltration of macrophages to the injured area and is belatedly able to restore muscle GH levels for nociceptor signaling prior to full sensitization. Further, previous reports indicate that the use of free GH by macrophages is necessary for proper immune function such as control over their production of cytokines and growth factors which subsequently regulates the inflammatory response to injury (Lu et al., 2013). Here, we found that the prevention of GH signaling to macrophages by specific deletion of the GHr in these cells resulted in a reduced control over injury-site specific cytokine levels (Fig. 4) (Lu et al., 2013) (Kumar et al., 2014). It is

worth noting that recent work has indicated an opposite effect, demonstrating that activating macrophages in culture with GH also results in an increased pro-inflammatory cytokine release (Schneider et al., 2019). It is likely that GH signaling is used by these effector cells as a homeostatic regulator (Dehkhoda et al., 2018). Despite the increase of these factors known to be pro-nociceptive (Sommer and Kress, 2004), our manipulation, which resulted in rescued muscle GH levels, prevented sensitization and pain-like behaviors. Interestingly, we also detected that the receptors of some cytokines, such as the IL1β receptor, are downregulated in DRG after a neonatal injury which may account for this discrepancy (Table 1). Also, it may be that restoration of GH signaling in neurons supersedes pro-nociceptive cytokine signaling (Figs. 1, 2, 5). It will be important to test this notion in the future.

Beyond acute sensitization, it has become clear that early life injury induces neuronal and immunological alterations that, when re-activated by an insult later in life, results in enhanced pain-like outcomes (Ren et al., 2004) (Boissé et al., 2005) (Walker et al., 2009) (Schwaller et al., 2015) (Moriarty et al., 2019) (Zhong et al., 2018). While a number of analyses of the central nervous and immune system have confirmed that this “priming” effect requires central processing, it is clear that primary afferent input is also necessary (Moriarty et al., 2019) (Beggs et al., 2012) (Walker et al., 2016) as opioid treatment could not alter neonatal priming responses but sciatic nerve block could (Moriarty et al., 2018). As our current (Fig. 2) and previous work (Liu et al., 2017) suggested that peripheral GH signaling regulated afferent sensitization and pain-related behaviors after injury, we posited that GH may also influence the “priming” effects that neonatal injury has on adolescent responses to re-injury. GH deficiency which induces a neonatal specific hypersensitivity to peripheral stimuli (Ford et al., 2019) is sufficient to prolong the normal behavioral responses to surgical insult similar to the repeated injury model (Fig. 5). Our reports are supported by a recent finding that shows in a different model of growth hormone deficiency, that animals are overall similar at adult baseline levels, however, are hypersensitive

following a hindpaw formalin challenge (Leone et al., 2019). These data suggest that GH levels and immune modulation are important for the induction of the early life injury “priming” effect and that this system can be manipulated by exogenous GH treatment.

Here, we describe a potentially neonatal specific mechanism of nociception as well as an intervention that is effective at blocking pain-like behaviors and primary afferent sensitization. Correlations between the level of circulating growth hormone levels and pain in patients has been previously observed in patients deficient in the hormone (Cimaz et al., 2001). Interestingly, patients that suffer from widespread muscle pain (fibromyalgia) sometimes also have altered GH levels and can be treated with GH supplements for pain. These results may have important clinical implications as many children are not diagnosed with growth hormone deficiency until they are a few years of age, in which time they may have already induced a “priming” effect to later in life injuries such as surgery. Together with the current and previous work (Liu et al., 2017), data suggest that interventions designed to control the local levels of GH may be clinically beneficial for pain in children.

Methods

Animals. Male and female mice that were postnatal day 7 (P7) to P14 (+/- 1d around the specified age range) or P35-P56 were used throughout all experiments. In all cases except for experiments regarding SRF knockdown, no sex differences were observed and thus data is combined from both males and females for ease of presentation. Neonatal animals were kept with the dam and only separated for short durations at a time (<1.5hrs) to perform behavioral experiments. All mice were kept in an environment-controlled facility at Cincinnati Children's Hospital Medical Center with free access to food and water while on a 12-hour light/dark cycle. Animals are defined as wildtype (WT) controls, heterozygous (+/-), or homozygous (-/-) for the genetic manipulation throughout all experiments.

Swiss Webster mice were born in house or purchased from Charles River (Wilmington, MA) or Envigo (Indianapolis, IN) and were used as an outbred strain for most experimentation. Littermate and non-littermate C57BL/6 animals born in-house were used as controls for genetic lines bred on that background. A deletion of the growth hormone receptor (GHr) specifically on macrophages was kindly gifted to use by Dr. Ram Menon (University of Michigan). This mouse was generated by crossing a LysM-Cre positive animal (see Jax Stock#: 004781) with a GHr floxed animal to induce cell type specific genetic deletion of GHr in monocytes/macrophages. Animals with a knockout of the growth hormone releasing hormone receptor (GHRHr) were purchased from The Jackson Laboratory (C57BL/6J-Ghrhr^{lit}/J; Stock#: 000533). We developed a sensory neuron specific deletion of GHr by crossing a tamoxifen inducible Cre recombinase driven by the Advillin (Adv) promotor purchased from The Jackson Laboratory (Advillin-CreERT2; Stock#: 026516). Mice were crossed in-house with cryo-recovered (CCHMC Transgenic Core Facility) GHr floxed (GHr$^{tm1b(KOMP)Wtsi}$) embryos purchased from the KOMP Repository (Design ID#: 49728) to make an inducible sensory neuron specific GHr knockout (Adv;GHr$^{f/f}$). A Cre dependent reporter mouse was also used to drive tdTomato (tdTOM)

expression (B6.Cg-Gt(ROSA)26Sor$^{tm14(CAG\text{-}tdTomato)Hze}$/J) and was purchased from The Jackson Laboratory (Stock#: 007914). Finally, LysM-Cre animals purchased from The Jackson Laboratory (Stock#: 004781) were crossed to the tdTom mice to generate myeloid/macrophage reporter mice. All procedures were approved by the CCHMC Institutional Animal Care and Use Committee in compliance with AALAC approved practices.

Behavioral Measures: Neonatal animals (P7-P14) were transferred from their home cage to opaque chambers with a translucent lid and acclimated in a temperature-controlled environment for 10 minutes prior to assessments. Adolescent animals ($\geq$P35) were transferred to raised translucent boxes with a grid mesh bottom and acclimated for 25 minutes prior to data collection. After habituation, behavioral experiments followed including spontaneous paw guarding assessment, muscle mechanical withdrawal thresholds, cutaneous mechanical withdrawal thresholds, grip strength and/or proprioceptive behaviors. No cohort received more than two of the listed behaviors at a time to reduce stress and maternal separation time for neonatal animals. Data was obtained at baseline, 1d and/or 3d, or up to 21d for adolescent animals, post injury as indicated.

Spontaneous paw guarding assessments scores preferential weight bearing on a scale of zero to two, where zero is no guarding after injury, 1 indicates shifted weight bearing but the paw still touches the floor and 2 indicates full paw lifting. Assessments were made for a duration of 1 minute. Neonatal animals were scored every five minutes for 30 minutes, and adolescent animals were scored for an hour.

Hind paw muscle withdrawal was assessed with a digital Randall Selitto device (IITC Life Science Inc. Woodland Hills, CA, USA) with a dulled probe attachment ~2 mm wide at the tip. The dorsal paw was supported by the upper machine arm and the medial plantar paw was

slowly pressed with the dulled probe until a robust withdrawal response was evoked. The gram force that elicited a withdrawal response was considered threshold. Three trials were obtained at least five minutes intervals and averaged together for analysis. Maximum squeezing force was 150g for neonates and 350g or 500g for adolescent mice of different strains.

Cutaneous mechanical withdrawal thresholds were assessed on the dorsal surface of the hindpaw as described in previous reports (Liu et al., 2017) (Jankowski et al., 2014) (Marsh et al., 1999) for neonatal animals using an increasing series of calibrated von Frey filaments ranging from 0.07g to 6g. Threshold to withdrawal was determined in three trials with five minutes intervals between trials and averaged.

Dynamic paw muscle strength was assessed by neonatal hanging time (Au - Feather-Schussler and Au - Ferguson, 2016). Animals were held with forepaws near a thin metal rod spanning a 9.5 cm diameter apparatus until the rod was gripped. Animals were timed while freely hanging above a 12 cm padded drop until they released the bar, escaped the apparatus by climbing out, or 60 seconds was reached. An escape was determined to require enough muscle strength to pull up and out of the apparatus and was thus set to maximum time. Three trials were recorded and averaged.

To evaluate proprioception, we recorded the animals' innate righting reflex (Dallman and Ladle, 2013). Animals were gently turned over and placed on their back. The time to flip over to all four limbs was recorded and averaged over three trials with 5-minute intervals between trials.

Animals were weighed and their temperature was taken after an injection of growth hormone to determine if any GH-related side effects were present with our injection strategy. 24 hours after an intramuscular hindpaw injection, animals were weighed on a tabletop scale and their

temperature was recorded using a digital surface contact thermometer pressed against the chest of the anesthetized animal according to previous methods (Liu et al., 2017) (Goodrich, 1977).

Injections. Growth hormone was injected directly into the hind paw muscles in uninjured mice or in animals receiving incision injury. Experiments in Fig. 5c were intraperitoneal GH injections. Dosing ranged from 0.1mg/kg to 1.5 mg/kg in 10 µL for all neonatal experiments. Adolescent animals were injected with the 1.5mg/kg dose in 18 µL. 5mg/kg GH binding protein (GHBP) or vehicle (0.1% bovine serum albumin (BSA)) in PBS was injected in 10 µL into the hindpaw muscle. To induce Cre-recombinase in AdvGHr animals, tamoxifen was made fresh at 25mg/mL in corn oil and uninjured animals were singly injected intraperitoneal (i.p.) at P7 at a dose of 250mg/kg tamoxifen (Hester and Danzer, 2013).

Surgical Hind Paw Incisions. Animals were anesthetized with 2-3% isoflurane and a longitudinal incision of the right hairy hind paw skin was made lateral to the main saphenous nerve innervation territory. Then incision was continued in between the bones through to the flexor digitorum brevis muscles. Blunt manipulation of the muscle was performed using #5 forceps, but the plantar skin was left untouched. Prior to wound closing with 7-0 sutures, interventions corresponding to the experiment were injected into the incision site. When appropriate, adolescent surgical hind paw incisions were performed using the same procedures, with wounds closed with 6-0 sutures. Animals were allowed to recover for the indicated times. For comparisons, some cohorts only received the hairy skin incision or a single suture through intact skin (sham) but did not experience the muscle incision. For dual incision assays, similar procedures were followed as described above except the first incision was made at P7 and the second incision (when indicated) was performed at P35.

Sciatic Nerve Injections. Mice were placed on a warming pad and kept under 2-3% isoflurane anesthesia as the right sciatic nerve was revealed by a small incision of the skin and cautious separation of the underlying muscle. Carefully, as to not stretch the nerve, the sciatic was separated from surrounding tissue and raised onto a malleable plastic platform. Targeting or control siRNAs were injected directly into the sciatic nerve above the trifurcation using quartz microelectrodes connected to a picospritzer with 8-10 short pulses at 1-2psi. Approximate volume of injection was ~100nL. 4 different duplexes from ON-TARGETplus SMARTpool siRNAs (Dharmacon, Lafayette; Catalog#: 4390771) against serum response factor were first tested *in vitro* (Neuro2a cells) to determine knock down efficiency of the individual siRNA duplexes similar to previous reports [e.g.] (Queme et al., 2016) (Ross et al., 2016) (Liu et al., 2017) (data not shown). The most efficient sequence was determined using realtime PCR and used for all subsequent *in vivo* analyses (sense: 5'-S-S-GCAGCAACCUCACCGAGCUUU; antisense: 5'-P-AGCUCGGUGAGGUUGCUGCUU). siRNAs were first conjugated to Penetratin-1 according to manufacturer's instructions after thiol removal (Dharmacon) and reconstituted at 90µM. Depending on age, siRNAs were then injected into the sciatic nerve as described above one (<P10) or two (≥P10) days prior to incision and further experimentation to allow for retrograde transport of the siRNAs to the DRG somas. The non-coding control siRNA has been used previously and does not target any murine gene (ThermoFisher D-001206-14-05).

Realtime RT-PCR. RNA was isolated from lumbar 3/4/5 (L3/4/5) dorsal root ganglia (DRG) on the side ipsilateral to injury. RNeasy Mini Kit (Qiagen Stock#: 74104) was performed on DRGs for total mRNA isolation and RNeasy Fibrous Tissue Mini Kit (Qiagen Stock#: 74704) was used to isolate muscle mRNA. All RNA isolations were performed exactly according to the manufactures directions. For standard realtime PCR assessments, 500ng of total RNA was reverse transcribed into cDNA and realtime PCR performed using SYBR Green Master Mix on a

StepOne realtime PCR system (Applied Biosystems). Quantitative PCR was analyzed by the ΔΔcycle threshold (CT) method with normalization to GAPDH. Fold change between conditions was determined and converted to a percent change where 2-fold = 100% change. Primer sequences are all recorded (Suppl. Table 2).

Western Blot. Flexor digitorum brevis muscle or L3/4/5 DRGs were dissected and frozen on dry ice. After homogenization in protein lysis buffer as completed previously [e.g.] (Ross et al., 2018), 20 µg samples were boiled in gel loading buffer containing β-mercaptoethanol as a reducing agent and loaded onto a 12% or "AnyKD" precast polyacrylamide gel (Bio-Rad 4569033) for western blot analysis. Gels were transferred to a polyvinylidene difluoride membranes (PVDF; Merck Millipore Ltd., Tullagreen, Ireland) at 35V for 16-18 hours at 4ºC. The next day, transfer quality was assessed by staining (Coomassie Brilliant Blue BioRad 1610436) the gel for any remaining proteins. The membrane was washed, blocked with Odyssey Blocking Buffer (BB) (LiCor 927-40000) diluted in PBS (1:4), and incubated in 2x PBS with 0.2%Tween and BB (1:1) with primary antibodies. After incubation overnight, the membranes were washed, incubated in 2x PBS with 0.2%Tween and 0.01% SDS and BB (1:4) with appropriate infrared-conjugated secondary antibodies (LiCor) and visualized on LiCor Odyssey CLx protein imaging system. Exposure times were consistent between runs and gain was always set to 1.0. Band intensity was then quantified using ImageJ software (NIH) similar to previous procedures (Liu et al., 2017). Primary antibodies included GH (LS-C146263, polyclonal rabbit, 1:1,000) and GAPDH (Abcam 83956, polyclonal chicken, 1:2,000).

***Immunohistochemistry*.** DRGs, sciatic nerve and hindpaw muscle were sectioned on a cryostat at 10 µm (DRG and sciatic nerve) or 20 µm (muscle). DRGs were frozen on dry ice in OCT medium and muscle was snap frozen in liquid nitrogen. All tissue was kept at -80°C until use. Cryostat sections were then fixed on the slide. Slides were washed and blocked prior to

overnight primary antibody incubation. The next day, the tissue was washed and stained for secondary antibodies before cover slipping with mounting media containing DAPI to mark nuclei (Fisher Scientific 17985-50). For immunocytochemistry, samples were processed by Cincinnati Children's Pathological core. Briefly, slides were pretreated with citrate buffer, washed and incubated with primary antibody for 32 minutes. Detection was completed with the DAB rabbit kit (Ventana#: 760-151), counterstained with hematoxylin and blued with bluing reagent, and then dehydrated before coverslipping. Primary antibodies used were: GH (LS-C146263, polyclonal rabbit, 1:500 (fluorescence) or 1:100 (DAB)), GHr (Abcam 202964, polyclonal rabbit, 1:1,000), SRF (Abcam 53147, polyclonal rabbit, 1:250), and dystrophin (Abcam 15277, polyclonal rabbit, 1:250). Fluorescent imaging was observed on a Nikon confocal microscope and all gain and laser power were maintained equally across all samples in each experiment. For quantification, images were converted to grayscale by a blind investigator and an equal threshold was applied to all images. A 200x200 region of interest (ROI) defined by positive staining was analyzed for particles of sufficient size and were quantified for mean gray value (ImageJ User Guide).

To quantify myofiber cross sectional area, we used the protocol established by Nikolaou and colleagues (Nikolaou et al., 2015). Briefly, dystrophin stained sections of hindpaw muscle were acquired on the Nikon confocal microscope at high intensity to obtain consistent signal around myofibers. Images were captured using NIS Elements software and then using Fiji software (Schindelin et al., 2012), images were converted to 8-bit binary images. Converted images were then manually edited to remove non-muscle regions or damaged fiber staining. Myofiber cross-sectional area measurements were then obtained for each fiber in the section. Three non-consecutive sections per condition were analyzed and averaged.

***Ex vivo* Preparation.** A novel neonatal *ex vivo* hind paw muscle-tibial nerve-DRG-spinal cord recording preparation was used to directly assess the response properties of individual primary

afferent neurons under our various conditions. Briefly, based on the forepaw prep previously described (Queme et al., 2020), animals were first anesthetized with a mix of ketamine and xylazine (100 and 16 mg/kg, respectively) and then perfused with ice cold oxygenated (95%O_2 /5% CO_2) artificial cerebral spinal fluid (aCSF; in mM: 127.0 NaCl, 1.9 KCl, 1.2 KH2PO4, 1.3 MgSO4, 2.4 CaCl2, 26.0 NaHCO3, and 10.0 D-glucose). The intact spine and right hind leg were isolated and transferred to a new dish with circulating oxygenated aCSF. The hind paw muscle (with bone intact), tibial/sciatic nerve, L1-L6 DRGs and corresponding spinal cord segments were dissected in continuity. The spinal cord was hemisected, and the intact preparation was then transferred to a new recording chamber under the same conditions. The paw with revealed muscle was pinned to a metal grate within an inner bath under its own circulation of O_2aCSF. The nerve was fed through a small gap of the inner bath and the spinal cord and DRGs were pinned within the outer dish. The hole between the dishes was filled with petroleum jelly to separate the baths and hold the nerve in place. The bath was slowly warmed to 32ºC.

Quartz microelectrodes (impedance>150MΩ) containing 5% Neurobiotin (Vector Laboratories, Burlingame, CA) in 1M potassium acetate were used for sharp electrode single unit recordings in the L3 or L4 DRGs. An impaled cell body was determined to have axons in the tibial nerve by a response from electrical search stimulus by a suction electrode placed on the side of the nerve. Once a cell was determined to have axons in the tibial nerve, the muscle was probed with concentric bipolar electrode to locate the cell's receptive field (RF) in the hindpaw muscle. Then the muscle was probed with mechanical stimuli, thermal stimuli and chemical stimuli in this order. For mechanical stimuli, an increasing series of von Frey filaments ranging from 0.07-10 grams were used to stimulate the RF for ~1-2s. Then cold (~2ºC) followed by hot (~53ºC) physiological saline was delivered to the RF. Following the thermal stimulations, two distinct metabolite mixtures were slowly introduced into the inner bath surrounding the hind paw

muscles. First a “low” concentration of metabolites (15 mM lactate, 1 μM ATP, pH 7.0) were applied for approximately two minutes and then washed out. After washout, a “high” concentration of metabolites (50 mM lactate, 5 μM ATP, pH 6.6) was added to the inner chamber in the same manner. Metabolites were oxygenated and heated to physiological conditions with an in-line heater to maintain bath conditions. ATP was added just before perfusion of the muscle. After metabolite stimulation, mechanical and thermal responsiveness was again assessed.

All activity was recorded by Spike2 software (Cambridge Electronic Design) and was later analyzed offline. Response latencies were recorded and divided by nerve length to determine conductance velocities to categorize group IV afferents (≤1.2 m/s) or group III afferents (1.2-14 m/s). Mechanical thresholds were determined by the least amount of force necessary to elicit at least two action potentials. Peak instantaneous frequencies (IF) were determined to assess the maximum response to a peripheral stimulus while firing rates (FR) were determined to obtain the maximum number of events that occurred over a given period of time (200ms bins). The distribution analyses were determined to be the number of cells that responded to a given stimuli divided by the number of total cells receiving that stimulus. Since chemical stimulation was not given to every cell tested, the distribution of each subtype of chemically activated cells (low, high or both) was divided by total chemically responsive cells per condition. No differences in response properties were found between cells obtained at the beginning of a recording experiment compared to the end of the session.

Statistics. Data were analyzed using SigmaPlot software (v.14). Critical significance was set to $\alpha<0.05$ and all claims of no effect are supported by power $\beta>0.8$. All data was first checked for normal distribution with Shapiro-Wilk and equal variance with Brown-Forsythe and then parametric or nonparametric tests were used accordingly. Specific tests are indicated in the

figure legends. For behavioral data containing the same animals treated with an intervention over time, a two-way repeated measures analysis of variance (RM ANOVA) was used. In behavioral data in which only one time point or a percent change from baseline/naïve was compared across groups a one-way ANOVA was used. Analysis of cDNA, protein quantification, area under the curve, or *ex vivo* analysis was measured by a one-way ANOVA or corresponding non-parametric test across groups. All analyses that passed the omnibus F-test were further discriminated by Tukey's, Holm-Sidak, or Dunn's post hoc analysis as noted in figure legends. Discrete categorical data were analyzed by chi-square across all groups. Graphical panels were made using Graphpad Prism (v.8) and compiled in Adobe Photoshop. In all studies involving subjective measures including all behavior, *ex vivo* and IHC quantification, the researcher was blinded by co-investigators or by the unknown genotype of the animal. The rare occasion of a detected outlier defined as being greater than 2 standard deviations away from the mean was removed. Biological replicates ("n") are provided for each figure in the legends or text. Technical replicates are explained above for each experiment.

Author contributions:

A.J.D. and M.P.J. conceived and designed the study and completed the *ex vivo* experiments and analysis. A.J.D. collected most of the data and completed the analyses. Z.K.F., K.J.G. and C.E.M. collected 1d MacGHrKO, clodronate, some GH-treatment, GHBP, and WT dual incision data. M.H. and R.C.H. managed the colony and performed genotyping assays in addition to performing some immunohistochemical and cell culture experiments.

Acknowledgements: This work was supported by grants to MPJ from the NIH (R01NS105715, R56NS103178) and the Rita Allen Foundation in addition to support from the Cincinnati Children's Research Foundation and Department of Anesthesia. We would also like to thank Dr. Ram Menon from the University of Michigan for supplying us with the macrophage specific GH receptor knockout mice.

Figure Legends:

Figure 1: Modulation of neonatal nociception by peripheral GH signaling.
a, Animals injected with GHBP display increased paw guarding at 1d compared to BL while vehicle injected animals do not and guard significantly more than vehicle injected groups. * indicates p<0.001 vs. BL and p<0.05 vs. Day 1 control. n = 12/group, Two-way RM ANOVA, Tukey's post hoc. b, Representative genotyping analysis of Adv-Cre; $GHr^{f/f}$ mice. b',b'', Immunostaining of DRGs for GHr (red) and nuclear labeling using DAPI (blue) in tamoxifen treated control (Adv;$GHr^{+/f}$) and Adv;$GHr^{f/f}$ mice. Arrows indicate GHr+ neuronal staining, large arrow indicates nerve fiber. c, Righting reflexes are not different across groups at 5- and 7-days post tamoxifen. n = 11-14 (GHr+/+), 26-30 (GHrf/+), 26-29 (GHrf/f), 13-16 (Adv;GHrf/+), and 5-7 (Adv;GHrf/f)/time point, Two-way RM ANOVA, Tukey's post hoc. d, Cutaneous mechanical withdrawal thresholds increased over time in control groups but not in Adv;$GHr^{f/+}$ (n = 8-12/time point) nor Adv;$GHr^{f/f}$ (8-10/time point) animals. *p<0.001 vs. BL; ^p<0.05 vs. each control group. Two-way RM ANOVA, Tukey's post hoc. d', Combined mutant (Adv;$GHr^{f/+}$, Adv;$GHr^{f/f}$) groups have significantly lower cutaneous mechanical withdrawal thresholds compared to control groups ($GHr^{+/+}$, $GHr^{f/+}$, $GHr^{f/f}$, n=6-7, 16-22, 10-14/time point respectively) in an area under the curve from BL (P7) to 7d (P14) post tamoxifen. #p<0.001 vs. controls. One-way ANOVA, Tukey's post hoc. e, In the same animals that received cutaneous stimulation, muscle mechanical thresholds increased over time in all groups. *p<0.001 vs. BL, Two-way RM ANOVA, Tukey's post hoc. e', Area under the curve analysis for muscle mechanical thresholds in combined groups indicates a reduced threshold in GHr mutant groups compared to controls. #p=0.002 vs. controls. One-way ANOVA, Tukey's post hoc. f, Dynamic muscle strength indicated that all groups except Adv;$GHr^{f/f}$ increased over time by 7 days post tamoxifen. *p<0.001 vs. BL. n = same as (c). f', Combined group area under the curve analysis reveals significantly reduced time in mutant GHr groups (n = 18-23/time point) compared to control groups (n = 65-70/time point). #p<0.001 vs. controls, one-way ANOVA, Tukey's post hoc. Data shown as mean ± s.e.m.

Figure 2: Intramuscular growth hormone injection inhibits peripheral sensitization in neonates with incision.
a, Representative image and analysis of muscle growth hormone (GH) levels using western blot. Following incision, growth hormone levels are reduced in incised animals compared to naïve animals and this is restored with exogenous GH treatment. *p<0.05 vs. naïve. n = 3/group, one-way ANOVA, Tukey's post hoc. b, Spontaneous paw guarding is increased following incision in animals treated with vehicle but not in GH treated animals at one day. By three days, neither group is different from their baseline (BL) or each other. *p<0.001 vs. BL; ^p<0.001 vs. control. n = 8-10/group, two-way RM ANOVA, Tukey's post hoc. c, Muscle withdrawal thresholds are reduced in incised animals with vehicle injection at 1d, but this is inhibited in GH treated animals. By three days, both groups have increased withdrawal thresholds compared to baseline. *p<0.05 vs. BL. n = 8-10/group, two-way ANOVA, Tukey's post hoc. d, When GH treatment is delayed eight hours following the injury, both groups are increased from their BL, but GH treated animals guard their paw significantly less than vehicle treated controls. *p<0.01 vs. BL, ^p<0.01 vs. control. n = 10/group, two-way RM ANOVA, Tukey's post hoc. e, Representative image of the hind paw muscle *ex vivo* recording preparation. f, Prevalence of mechanically and chemically ("low", "high", or "both") sensitive muscle afferents are altered by incision and rescued by GH treatment. *p<0.05 vs naïve, $\square^2$. g, von Frey threshold of mechanically sensitive group III/IV primary afferents. Compared to naïve animals (n = 6 animals, 51 cells), surgical injury results in sensitization in incised animals (n = 8 animals, 50 cells) that is blocked by GH treatment (n = 10 animals, 54 cells). h, The average mechanical firing rate is decreased in injured animals treated with GH compared to those that

were not treated after injury. *p<0.05 vs naïve. ANOVA on Ranks, Dunn's post hoc. i, Representative mechanical responses for each group are provided. Data shown as mean ± s.e.m.

Figure 3: Nerve-targeted knockdown of SRF upregulation blunts pain-like responses after muscle incision.
a, Injection if SRF targeting siRNAs (PenSRF) into the sciatic nerve reduces the upregulation of SRF mRNA in the DRGs after hind paw incision compared to incised mice injected with control siRNAs (PenCON). *p<0.001 vs. naïve, ^p<0.05 vs. PenCON. n = 7 naïve, 22 PenCON, 19 PenSRF, one-way ANOVA, Holm-Sidak post hoc. b, Representative images (bi-ii) display similar results at the protein level, arrows indicate SRF+ staining, big arrow indicates satellite cell, (b') using immunocytochemical labeling and mean staining value of a ROI (red). DAPI (blue) co-stain was used to mark all nuclei. *p<0.05 vs. PenCON. n = 3 animals/group, Tukey's post hoc. c, Incised animals show increased paw guarding over time, and animals injected with PenSRF showed reduced guarding compared to the PenCON injected mice. d, PenCON incised animals have reduced mechanical withdrawal thresholds compared to baseline, and PenSRF animals display significantly less reduction compared to PenCON injected animals. *p<0.05 vs BL, ^p<0.05 vs. PenCON. n = 15-16/group, two-way RM ANOVA, with Tukey's post hoc. Data shown as mean ± s.e.m or percent change from naïve.

Figure 4: Muscle growth hormone distribution is altered by injury and macrophage specific GHr knockout attenuates pain-like phenotypes.
a, Immunostaining for GH (arrows) in a cross section of hindpaw muscle of a naïve animal with DAB (3,3′-Diaminobenzidine) staining. b, GH staining (arrows) in the muscle of an animal 1d after an incision. c, Overlay of macrophages and GH (arrows) in the muscles of a LysMcre/tdTomato reporter animal using an antibody stain for GH (green) (c') and tdTom reporter for macrophages (red) (c'') one day after an injury of the hindpaw muscle. d-d'' Representative higher magnification images of macrophage and GH overlay (arrows) in injured muscle. e, Representative image of GH staining (dashed arrow) using DAB in the muscles of an injured macrophage specific growth hormone receptor knockout (MacGHr-/-) animal. Hematoxylin (light red) dense cells show infiltrating macrophages (solid arrows). e'-e'', Representative western blots and quantification of growth hormone levels after injury in MacGHr-/- animals. f, MacGHr knockout animals display less guarding compared to WT controls at 1d after injury, though both groups display increased guarding from baseline. g, MacGHr-/- mice do not show reduced muscle withdrawal thresholds after injury while WT controls display decreased thresholds. *p<0.05 vs. BL, ^p<0.05 vs. controls, #p=0.07 vs. BL. n = 12 - 13/group, one-way or two-way ANOVA, with Tukey's post hoc. h, Upregulation of select receptors/channels in the DRGs are observed in WT control mice with incision, but this is not found in incised MacGHr-/- DRGs. i, Incision-induced upregulation of select cytokines and growth factors in the muscles is found in both control and MacGHr-/- mice. *p<0.05 vs. naïve, ^p<0.05 vs. WT incised. n = 3-4/group, two-way ANOVA, Tukey's post hoc. Data shown as mean ± s.e.m or percent change from naïve.

Figure 5: Alterations in GH levels during early postnatal development modulate the behavioral responses to incision in adolescence. a, GHRHr-/- animals guard their injured limb to a greater degree and for a longer time after P35 incision compared to GHRHr+/- and WT controls (GHRHr+/+). b, Muscle mechanical hypersensitivity is also more severe and prolonged in GHRHr+/- and GHRHr-/- mice with incision at P35 compared to GHRHr+/+ animals. *p<0.05 vs. BL (indicated for each group by the colored horizontal bars next to the "*" for each group, the ending of the bar indicates the ending of the detected significance); ^p<0.05 vs. time-matched

GHRHr+/+; #p<0.001 vs. time-matched GHRHr+/-. n = 9-13/group, two-way RM ANOVA with Tukey's or ANOVA on Ranks with Dunn's post hoc. c, Muscle withdrawal thresholds in wildtype mice following a P7 plus P35 incision are prolonged compared to mice that only received a single injury at P35. This effect is blocked by injection of GH during P7 incision. *p<0.05 vs. BL (indicated as in "a" and "b". ^p<0.05 vs. time-matched P35 incision only. n = 11-12/group, two-way RM ANOVA, with Tukey's post hoc. Data shown as the mean ± s.e.m.

Figure 6: Role of GH in neonatal nociception. Under naïve conditions (left), GH is diffusely available throughout the neonatal muscle tissue, allowing persistent activation of the GHr on primary afferent nociceptors. Normal activation of neuronal GHr maintains homeostatic transcription levels and regulates sensitizing factors such as TRPA1 and TRPV1 partially through SRF-dependent regulation. Following a neonatal injury (right), macrophages infiltrate the injured tissue and sequester GH, thereby effectively reducing GH-availability to the nociceptors. The removal of tonic GH signaling to neurons permits SRF (and possibly STAT5) dependent transcription of various receptors and channels, leading to nociceptor sensitization and pain-related hypersensitivity after injury.

Tables:

Table 1: **Transcriptional changes following a neonatal muscle incision and local GH injection are modulated in L3/4/5 DRGs but not In the injured muscle.** Data shown as a percent change from controls. n = *p<0.05 vs. controls. n = 3-12/group, one-way ANOVA with Tukey's or ANOVA on Ranks, with Dunn's post hoc.

References

Adelman, P., Baumbauer, K., Friedman, R., Shah, M., Wright, M., Young, E., Jankowski, M.P., Albers, K.M., and Koerber, H.R. (2019). Single cell q-PCR derived expression profiles of identified sensory neurons. bioRxiv, 560672.

Au - Feather-Schussler, D.N., and Au - Ferguson, T.S. (2016). A Battery of Motor Tests in a Neonatal Mouse Model of Cerebral Palsy. JoVE, e53569.

Baccei, M.L. (2016). Rewiring of Developing Spinal Nociceptive Circuits by Neonatal Injury and Its Implications for Pediatric Chronic Pain. Children *3*, 16.

Baoge, L., Van Den Steen, E., Rimbaut, S., Philips, N., Witvrouw, E., Almqvist, K.F., Vanderstraeten, G., and Vanden Bossche, L.C. (2012). Treatment of skeletal muscle injury: a review. ISRN orthopedics *2012*, 689012.

Bartholomew EF, M.F., Nath JL. (2009). Fundamentals of anatomy & physiology. Upper Saddle River, NJ: Pearson Education Inc *616–617*.

Basbaum, A.I., Bautista, D.M., Scherrer, G., and Julius, D. (2009). Cellular and molecular mechanisms of pain. Cell *139*, 267-284.

Beggs, S., Currie, G., Salter, M.W., Fitzgerald, M., and Walker, S.M. (2012). Priming of adult pain responses by neonatal pain experience: maintenance by central neuroimmune activity. Brain *135*, 404-417.

Boissé, L., Spencer, S.J., Mouihate, A., Vergnolle, N., and Pittman, Q.J. (2005). Neonatal immune challenge alters nociception in the adult rat. Pain *119*, 133-141.

Brennan, T.J., Vandermeulen, E.P., and Gebhart, G.F. (1996). Characterization of a rat model of incisional pain. Pain *64*, 493-501.

Brewer, C.L., and Baccei, M.L. (2019). The development of pain circuits and unique effects of neonatal injury. Journal of neural transmission (Vienna, Austria : 1996).

Carter-Su, C., Schwartz, J., and Argetsinger, L.S. (2016). Growth hormone signaling pathways. Growth Horm IGF Res *28*, 11-15.

Ceseña, T.I., Cui, T.X., Piwien-Pilipuk, G., Kaplani, J., Calinescu, A.A., Huo, J.S., Iñiguez-Lluhí, J.A., Kwok, R., and Schwartz, J. (2007). Multiple mechanisms of growth hormone-regulated gene transcription. Molecular genetics and metabolism *90*, 126-133.

Cimaz, R., Rusconi, R., Fossali, E., and Careddu, P. (2001). Unexpected healing of cutaneous ulcers in a short child. Lancet (London, England) *358*, 211-212.

Cuatrecasas, G. (2009). Fibromyalgic syndromes: could growth hormone therapy be beneficial? Pediatric endocrinology reviews : PER *6 Suppl 4*, 529-533.

Cuatrecasas, G., Alegre, C., and Casanueva, F.F. (2014). GH/IGF1 axis disturbances in the fibromyalgia syndrome: is there a rationale for GH treatment? Pituitary *17*, 277-283.

Cuatrecasas, G., Alegre, C., Fernandez-Solà, J., Gonzalez, M.J., Garcia-Fructuoso, F., Poca-Dias, V., Nadal, A., Cuatrecasas, G., Navarro, F., Mera, A.*, et al.* (2012). Growth hormone treatment for sustained pain reduction and improvement in quality of life in severe fibromyalgia. Pain *153*, 1382-1389.

Cuatrecasas, G., Gonzalez, M.J., Alegre, C., Sesmilo, G., Fernandez-Solà, J., Casanueva, F.F., Garcia-Fructuoso, F., Poca-Dias, V., Izquierdo, J.P., and Puig-Domingo, M. (2010). High

prevalence of growth hormone deficiency in severe fibromyalgia syndromes. The Journal of clinical endocrinology and metabolism *95*, 4331-4337.
Cuatrecasas, G., Riudavets, C., Güell, M.A., and Nadal, A. (2007). Growth hormone as concomitant treatment in severe fibromyalgia associated with low IGF-1 serum levels. A pilot study. BMC musculoskeletal disorders *8*, 119.
Dallman, M.A., and Ladle, D.R. (2013). Quantitative analysis of locomotor defects in neonatal mice lacking proprioceptive feedback. Physiology & behavior *120*, 97-105.
Dattani, M., and Preece, M. (2004). Growth hormone deficiency and related disorders: insights into causation, diagnosis, and treatment. Lancet (London, England) *363*, 1977-1987.
Dehkhoda, F., Lee, C.M.M., Medina, J., and Brooks, A.J. (2018). The Growth Hormone Receptor: Mechanism of Receptor Activation, Cell Signaling, and Physiological Aspects. Front Endocrinol (Lausanne) *9*, 35.
Dubick, M.N., Ravin, T.H., Michel, Y., and Morrisette, D.C. (2015). Use of localized human growth hormone and testosterone injections in addition to manual therapy and exercise for lower back pain: a case series with 12-month follow-up. Journal of Pain Research *8*, 295-302.
Farris, G.M., Miller, G.K., Wollenberg, G.K., Molon-Noblot, S., Chan, C., and Prahalada, S. (2007). Recombinant rat and mouse growth hormones: risk assessment of carcinogenic potential in 2-year bioassays in rats and mice. Toxicological sciences : an official journal of the Society of Toxicology *97*, 548-561.
Ford, Z.K., Dourson, A.J., Liu, X., Lu, P., Green, K.J., Hudgins, R.C., and Jankowski, M.P. (2019). Systemic growth hormone deficiency causes mechanical and thermal hypersensitivity during early postnatal development. IBRO Reports *6*, 111-121.
Gomez, R., Kohler, D.M., Brackley, A.D., Henry, M.A., and Jeske, N.A. (2018). Serum response factor mediates nociceptor inflammatory pain plasticity. Pain reports *3*, e658.
Goodrich, C.A. (1977). Measurement of body temperature in neonatal mice. Journal of applied physiology: respiratory, environmental and exercise physiology *43*, 1102-1105.
Gouin, O., L'Herondelle, K., Lebonvallet, N., Le Gall-Ianotto, C., Sakka, M., Buhe, V., Plee-Gautier, E., Carre, J.L., Lefeuvre, L., Misery, L.*, et al.* (2017). TRPV1 and TRPA1 in cutaneous neurogenic and chronic inflammation: pro-inflammatory response induced by their activation and their sensitization. Protein & cell *8*, 644-661.
Govers, R., ten Broeke, T., van Kerkhof, P., Schwartz, A.L., and Strous, G.J. (1999). Identification of a novel ubiquitin conjugation motif, required for ligand-induced internalization of the growth hormone receptor. The EMBO journal *18*, 28-36.
Hermann, C., Hohmeister, J., Demirakca, S., Zohsel, K., and Flor, H. (2006). Long-term alteration of pain sensitivity in school-aged children with early pain experiences. Pain *125*, 278-285.
Hester, M.S., and Danzer, S.C. (2013). Accumulation of abnormal adult-generated hippocampal granule cells predicts seizure frequency and severity. J Neurosci *33*, 8926-8936.
Jankowski, M.P., McIlwrath, S.L., Jing, X., Cornuet, P.K., Salerno, K.M., Koerber, H.R., and Albers, K.M. (2009). Sox11 transcription factor modulates peripheral nerve regeneration in adult mice. Brain research *1256*, 43-54.
Jankowski, M.P., Ross, J.L., Weber, J.D., Lee, F.B., Shank, A.T., and Hudgins, R.C. (2014). Age-dependent sensitization of cutaneous nociceptors during developmental inflammation. Mol Pain *10*, 34.

Julius, D., and Basbaum, A.I. (2001). Molecular mechanisms of nociception. Nature *413*, 203-210.
Kao, D.J., Li, A.H., Chen, J.C., Luo, R.S., Chen, Y.L., Lu, J.C., and Wang, H.L. (2012). CC chemokine ligand 2 upregulates the current density and expression of TRPV1 channels and Nav1.8 sodium channels in dorsal root ganglion neurons. Journal of neuroinflammation *9*, 189.
Koerber, H.R., McIlwrath, S.L., Lawson, J.J., Malin, S.A., Anderson, C.E., Jankowski, M.P., and Davis, B.M. (2010). Cutaneous C-polymodal fibers lacking TRPV1 are sensitized to heat following inflammation, but fail to drive heat hyperalgesia in the absence of TPV1 containing C-heat fibers. Mol Pain *6*, 58.
Koerber, H.R., and Woodbury, C.J. (2002). Comprehensive phenotyping of sensory neurons using an ex vivo somatosensory system. Physiology & behavior *77*, 589-594.
Kumar, P.A., Chitra, P.S., Lu, C., Sobhanaditya, J., and Menon, R. (2014). Growth hormone (GH) differentially regulates NF-kB activity in preadipocytes and macrophages: implications for GH's role in adipose tissue homeostasis in obesity. Journal of physiology and biochemistry *70*, 433-440.
Kumar, S.K., and Bhat, B.V. (2016). Distinct mechanisms of the newborn innate immunity. Immunology letters *173*, 42-54.
Lau, J., Minett, M.S., Zhao, J., Dennehy, U., Wang, F., Wood, J.N., and Bogdanov, Y.D. (2011). Temporal control of gene deletion in sensory ganglia using a tamoxifen-inducible Advillin-Cre-ERT2 recombinase mouse. Mol Pain *7*, 100.
Leone, S., Chiavaroli, A., Recinella, L., Orlando, G., Ferrante, C., Marconi, G.D., Gasparo, I., Bitto, A., Salvatori, R., and Brunetti, L. (2019). Increased pain and inflammatory sensitivity in growth hormone-releasing hormone (GHRH) knockout mice. Prostaglandins & other lipid mediators, 106362.
Lim, Y., and Godambe, S. (2017). Prevention and management of procedural pain in the neonate: an update, American Academy of Pediatrics, 2016. Archives of disease in childhood Education and practice edition *102*, 254-256.
Liu, X., Green, K.J., Ford, Z.K., Queme, L.F., Lu, P., Ross, J.L., Lee, F.B., Shank, A.T., Hudgins, R.C., and Jankowski, M.P. (2017). Growth hormone regulates the sensitization of developing peripheral nociceptors during cutaneous inflammation. Pain *158*, 333-346.
Lu, C., Kumar, P.A., Sun, J., Aggarwal, A., Fan, Y., Sperling, M.A., Lumeng, C.N., and Menon, R.K. (2013). Targeted deletion of growth hormone (GH) receptor in macrophage reveals novel osteopontin-mediated effects of GH on glucose homeostasis and insulin sensitivity in diet-induced obesity. J Biol Chem *288*, 15725-15735.
Marsh, D., Dickenson, A., Hatch, D., and Fitzgerald, M. (1999). Epidural opioid analgesia in infant rats II: responses to carrageenan and capsaicin. Pain *82*, 33-38.
McMahon, S.B., Cafferty, W.B., and Marchand, F. (2005). Immune and glial cell factors as pain mediators and modulators. Exp Neurol *192*, 444-462.
McMahon, S.B., La Russa, F., and Bennett, D.L. (2015). Crosstalk between the nociceptive and immune systems in host defence and disease. Nature reviews Neuroscience *16*, 389-402.
Mendell, L.M. (1996). Neurotrophins and sensory neurons: role in development, maintenance and injury. A thematic summary. Philosophical transactions of the Royal Society of London Series B, Biological sciences *351*, 463-467.

Moqrich, A., Earley, T.J., Watson, J., Andahazy, M., Backus, C., Martin-Zanca, D., Wright, D.E., Reichardt, L.F., and Patapoutian, A. (2004). Expressing TrkC from the TrkA locus causes a subset of dorsal root ganglia neurons to switch fate. Nat Neurosci *7*, 812-818.
Moriarty, O., Harrington, L., Beggs, S., and Walker, S.M. (2018). Opioid analgesia and the somatosensory memory of neonatal surgical injury in the adult rat. British journal of anaesthesia *121*, 314-324.
Moriarty, O., Tu, Y., Sengar, A.S., Salter, M.W., Beggs, S., and Walker, S.M. (2019). Priming of Adult Incision Response by Early-Life Injury: Neonatal Microglial Inhibition Has Persistent But Sexually Dimorphic Effects in Adult Rats. The Journal of Neuroscience *39*, 3081.
Muller, E.E., Locatelli, V., and Cocchi, D. (1999). Neuroendocrine control of growth hormone secretion. Physiological reviews *79*, 511-607.
Nikolaou, S., Hu, L., and Cornwall, R. (2015). Afferent Innervation, Muscle Spindles, and Contractures Following Neonatal Brachial Plexus Injury in a Mouse Model. The Journal of hand surgery *40*, 2007-2016.
Philippou, A., Maridaki, M., Theos, A., and Koutsilieris, M. (2012). Cytokines in muscle damage. Advances in clinical chemistry *58*, 49-87.
Pinho-Ribeiro, F.A., Baddal, B., Haarsma, R., O'Seaghdha, M., Yang, N.J., Blake, K.J., Portley, M., Verri, W.A., Dale, J.B., Wessels, M.R.*, et al.* (2018). Blocking Neuronal Signaling to Immune Cells Treats Streptococcal Invasive Infection. Cell *173*, 1083-1097.e1022.
Queme, L.F., Ross, J.L., Lu, P., Hudgins, R.C., and Jankowski, M.P. (2016). Dual Modulation of Nociception and Cardiovascular Reflexes during Peripheral Ischemia through P2Y1 Receptor-Dependent Sensitization of Muscle Afferents. J Neurosci *36*, 19-30.
Queme, L.F., Weyler, A.A., Cohen, E.R., Hudgins, R.C., and Jankowski, M.P. (2020). A dual role for peripheral GDNF signaling in nociception and cardiovascular reflexes in the mouse. Proc Natl Acad Sci U S A *117*, 698-707.
Ren, K., Anseloni, V., Zou, S.P., Wade, E.B., Novikova, S.I., Ennis, M., Traub, R.J., Gold, M.S., Dubner, R., and Lidow, M.S. (2004). Characterization of basal and re-inflammation-associated long-term alteration in pain responsivity following short-lasting neonatal local inflammatory insult. Pain *110*, 588-596.
Ren, K., and Dubner, R. (2010). Interactions between the immune and nervous systems in pain. Nature medicine *16*, 1267-1276.
Ross, J.L., Queme, L.F., Cohen, E.R., Green, K.J., Lu, P., Shank, A.T., An, S., Hudgins, R.C., and Jankowski, M.P. (2016). Muscle IL1beta Drives Ischemic Myalgia via ASIC3-Mediated Sensory Neuron Sensitization. J Neurosci *36*, 6857-6871.
Ross, J.L., Queme, L.F., Lamb, J.E., Green, K.J., and Jankowski, M.P. (2018). Sex differences in primary muscle afferent sensitization following ischemia and reperfusion injury. Biology of sex differences *9*, 2.
Salaffi, F., Giacobazzi, G., and Di Carlo, M. (2018). Chronic Pain in Inflammatory Arthritis: Mechanisms, Metrology, and Emerging Targets-A Focus on the JAK-STAT Pathway. Pain research & management *2018*, 8564215.
Sass, F.A., Fuchs, M., Pumberger, M., Geissler, S., Duda, G.N., Perka, C., and Schmidt-Bleek, K. (2018). Immunology Guides Skeletal Muscle Regeneration. International journal of molecular sciences *19*.

Schindelin, J., Arganda-Carreras, I., Frise, E., Kaynig, V., Longair, M., Pietzsch, T., Preibisch, S., Rueden, C., Saalfeld, S., Schmid, B.*, et al.* (2012). Fiji: an open-source platform for biological-image analysis. Nat Methods *9*, 676-682.
Schneider, A., Wood, H.N., Geden, S., Greene, C.J., Yates, R.M., Masternak, M.M., and Rohde, K.H. (2019). Growth hormone-mediated reprogramming of macrophage transcriptome and effector functions. Scientific reports *9*, 19348.
Schwaller, F., Beggs, S., and Walker, S.M. (2015). Targeting p38 Mitogen-activated Protein Kinase to Reduce the Impact of Neonatal Microglial Priming on Incision-induced Hyperalgesia in the Adult Rat. Anesthesiology *122*, 1377-1390.
Sharma, N., Flaherty, K., Lezgiyeva, K., Wagner, D.E., Klein, A.M., and Ginty, D.D. (2020). The emergence of transcriptional identity in somatosensory neurons. Nature *577*, 392-398.
Shelton, D.L., and Reichardt, L.F. (1984). Expression of the beta-nerve growth factor gene correlates with the density of sympathetic innervation in effector organs. Proc Natl Acad Sci U S A *81*, 7951-7955.
Sommer, C., and Kress, M. (2004). Recent findings on how proinflammatory cytokines cause pain: peripheral mechanisms in inflammatory and neuropathic hyperalgesia. Neuroscience letters *361*, 184-187.
Strous, G.J., van Kerkhof, P., Govers, R., Ciechanover, A., and Schwartz, A.L. (1996). The ubiquitin conjugation system is required for ligand-induced endocytosis and degradation of the growth hormone receptor. The EMBO journal *15*, 3806-3812.
van der Lely, A.J., Hutson, R.K., Trainer, P.J., Besser, G.M., Barkan, A.L., Katznelson, L., Klibanski, A., Herman-Bonert, V., Melmed, S., Vance, M.L.*, et al.* (2001). Long-term treatment of acromegaly with pegvisomant, a growth hormone receptor antagonist. Lancet (London, England) *358*, 1754-1759.
Walker, S.M. (2019). Long-term effects of neonatal pain. Seminars in fetal & neonatal medicine.
Walker, S.M., apos, Reilly, H., Beckmann, J., and Marlow, N. (2018). Conditioned pain modulation identifies altered sensitivity in extremely preterm young adult males and female. BJA: British Journal of Anaesthesia *121*, 636-646.
Walker, S.M., Beggs, S., and Baccei, M.L. (2016). Persistent changes in peripheral and spinal nociceptive processing after early tissue injury. Experimental Neurology *275*, 253-260.
Walker, S.M., Tochiki, K.K., and Fitzgerald, M. (2009). Hindpaw incision in early life increases the hyperalgesic response to repeat surgical injury: critical period and dependence on initial afferent activity. Pain *147*, 99-106.
Weston, W.L., Carson, B.S., Barkin, R.M., Slater, G.D., Dustin, R.D., and Hecht, S.K. (1977). Monocyte-macrophage function in the newborn. American journal of diseases of children (1960) *131*, 1241-1242.
Winterberg, T., Vieten, G., Meier, T., Yu, Y., Busse, M., Hennig, C., Hansen, G., Jacobs, R., Ure, B.M., and Kuebler, J.F. (2015). Distinct phenotypic features of neonatal murine macrophages. European journal of immunology *45*, 214-224.
Ye, Y., and Woodbury, C.J. (2010). Early postnatal loss of heat sensitivity among cutaneous myelinated nociceptors in Swiss-Webster mice. Journal of neurophysiology *103*, 1385-1396.
Zhang, X., Azhar, G., Rogers, S.C., Foster, S.R., Luo, S., and Wei, J.Y. (2014). Overexpression of p49/STRAP alters cellular cytoskeletal structure and gross anatomy in mice. BMC Cell Biology *15*, 32-32.

Zhong, X.S., Winston, J.H., Luo, X., Kline, K.T., Nayeem, S.Z., Cong, Y., Savidge, T.C., Dashwood, R.H., Powell, D.W., and Li, Q. (2018). Neonatal Colonic Inflammation Epigenetically Aggravates Epithelial Inflammatory Responses to Injury in Adult Life. Cellular and molecular gastroenterology and hepatology *6*, 65-78.

Figure 1.

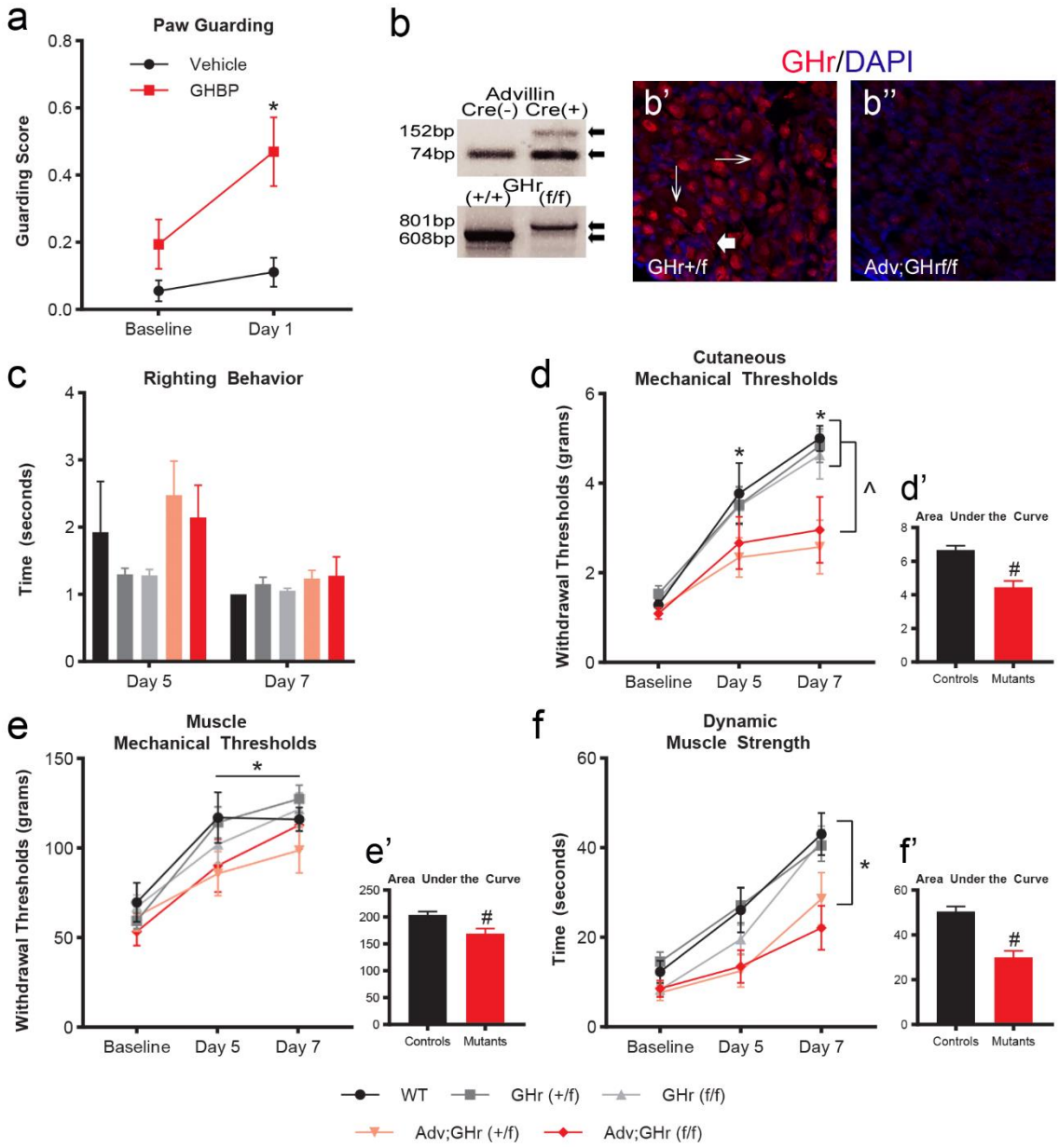
a
Paw Guarding
Vehicle
GHBP
Guarding Score
Baseline
Day 1
b
Advillin
Cre(-) Cre(+)
152bp
74bp
GHr
(+/+) (f/f)
801bp
608bp
GHr/DAPI
b'
b''
GHr+/f
Adv;GHrf/f
c
Righting Behavior
Time (seconds)
Day 5
Day 7
d
Cutaneous
Mechanical Thresholds
Withdrawal Thresholds (grams)
Baseline
Day 5
Day 7
d'
Area Under the Curve
Controls
Mutants
e
Muscle
Mechanical Thresholds
Withdrawal Thresholds (grams)
Baseline
Day 5
Day 7
e'
Area Under the Curve
Controls
Mutants
f
Dynamic
Muscle Strength
Time (seconds)
Baseline
Day 5
Day 7
f'
Area Under the Curve
Controls
Mutants
WT
GHr (+/f)
GHr (f/f)
Adv;GHr (+/f)
Adv;GHr (f/f)

Figure 2.

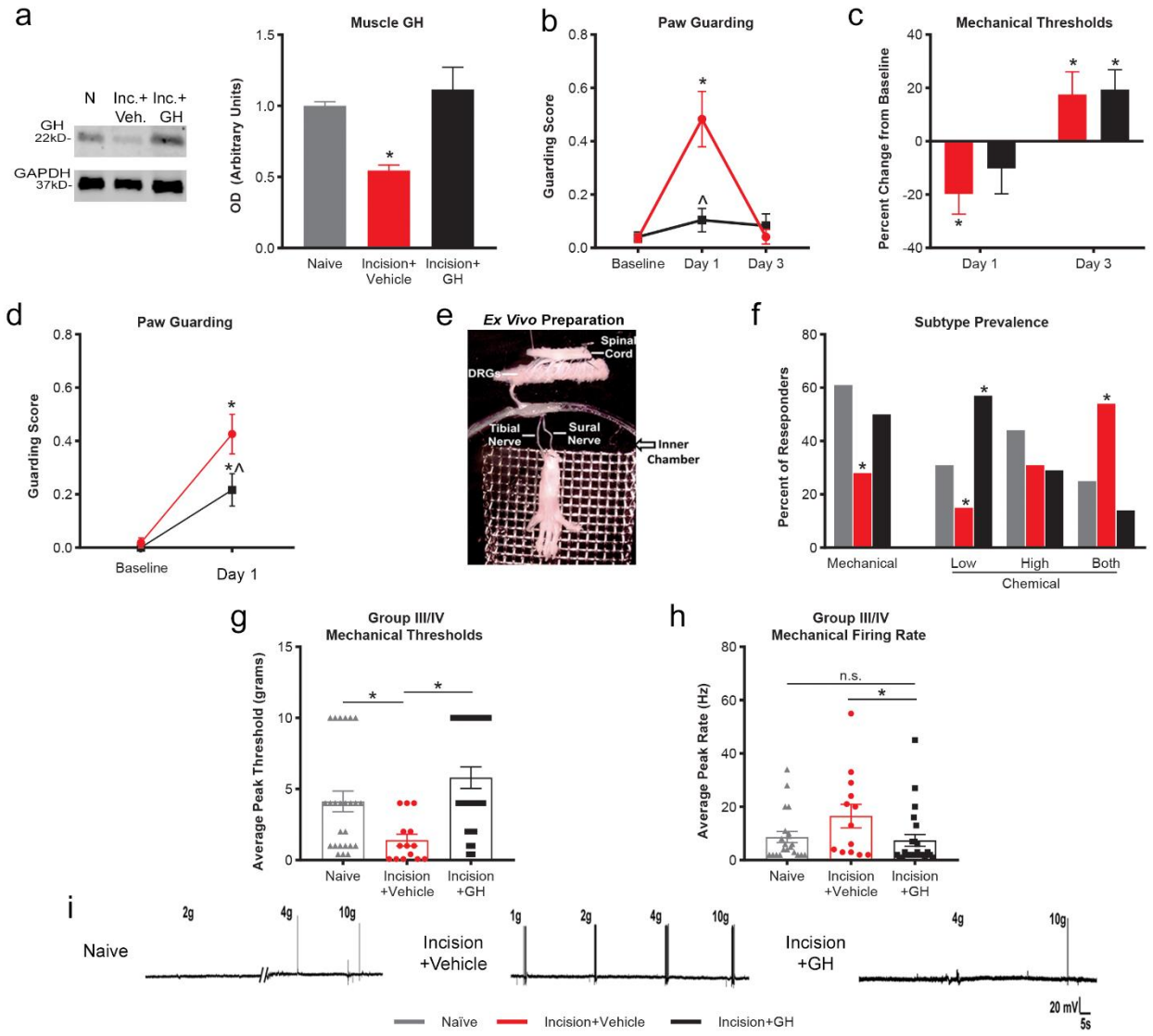
a
N
Inc.+ Veh.
Inc.+ GH
GH 22kD-
GAPDH 37kD-
Muscle GH
OD (Arbitrary Units)
Naive
Incision+ Vehicle
Incision+ GH
b
Paw Guarding
Guarding Score
Baseline
Day 1
Day 3
c
Mechanical Thresholds
Percent Change from Baseline
Day 1
Day 3
d
Paw Guarding
Guarding Score
Baseline
Day 1
e
Ex Vivo Preparation
Spinal Cord
DRGs
Tibial Nerve
Sural Nerve
Inner Chamber
f
Subtype Prevalence
Percent of Reseponders
Mechanical
Low
High
Both
Chemical
g
Group III/IV Mechanical Thresholds
Average Peak Threshold (grams)
Naive
Incision +Vehicle
Incision +GH
h
Group III/IV Mechanical Firing Rate
Average Peak Rate (Hz)
n.s.
Naive
Incision +Vehicle
Incision +GH
i
Naive
2g
4g
10g
Incision +Vehicle
1g
2g
4g
10g
Incision +GH
4g
10g
20 mV
5s
Naïve
Incision+Vehicle
Incision+GH

Figure 3.

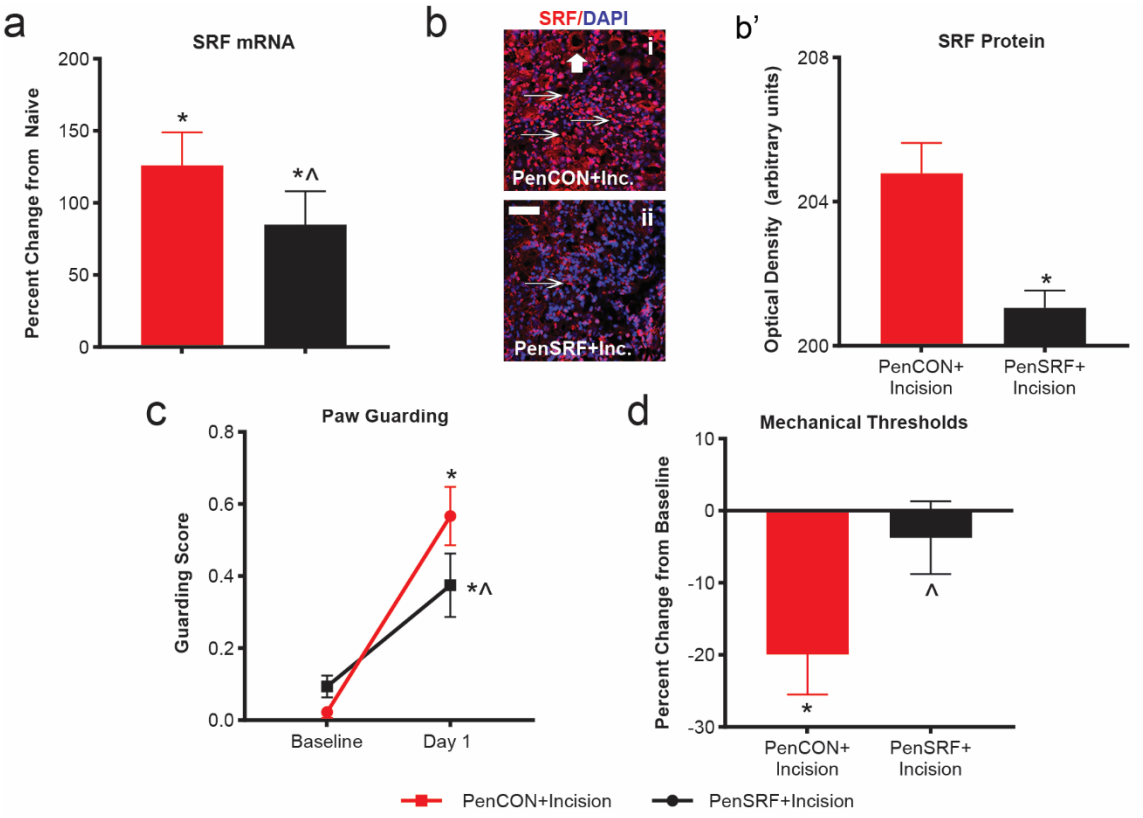
a
SRF mRNA
Percent Change from Naive
200
150
100
50
0
*
*^
b
SRF/DAPI
i
PenCON+Inc.
ii
PenSRF+Inc.
b'
SRF Protein
Optical Density (arbitrary units)
208
204
200
*
PenCON+ Incision
PenSRF+ Incision
c
Paw Guarding
Guarding Score
0.8
0.6
0.4
0.2
0.0
*
*^
Baseline
Day 1
d
Mechanical Thresholds
Percent Change from Baseline
10
0
-10
-20
-30
*
^
PenCON+ Incision
PenSRF+ Incision
PenCON+Incision
PenSRF+Incision

Figure 4.

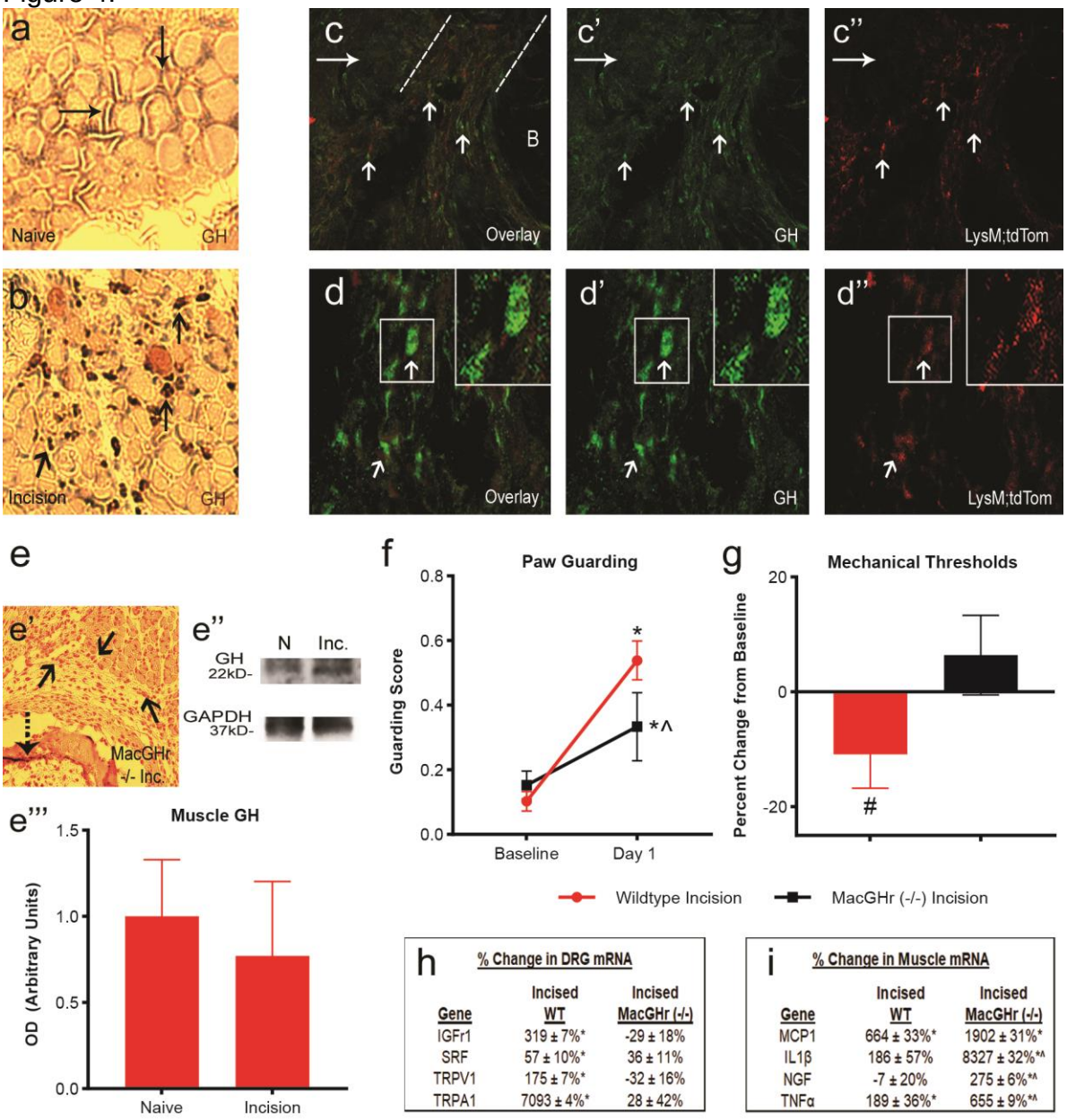

h **% Change in DRG mRNA**

Gene	Incised WT	Incised MacGHr (-/-)
IGFr1	319 ± 7%*	-29 ± 18%
SRF	57 ± 10%*	36 ± 11%
TRPV1	175 ± 7%*	-32 ± 16%
TRPA1	7093 ± 4%*	28 ± 42%

i **% Change in Muscle mRNA**

Gene	Incised WT	Incised MacGHr (-/-)
MCP1	664 ± 33%*	1902 ± 31%*
IL1β	186 ± 57%	8327 ± 32%*^
NGF	-7 ± 20%	275 ± 6%*^
TNFα	189 ± 36%*	655 ± 9%*^

Figure 5.

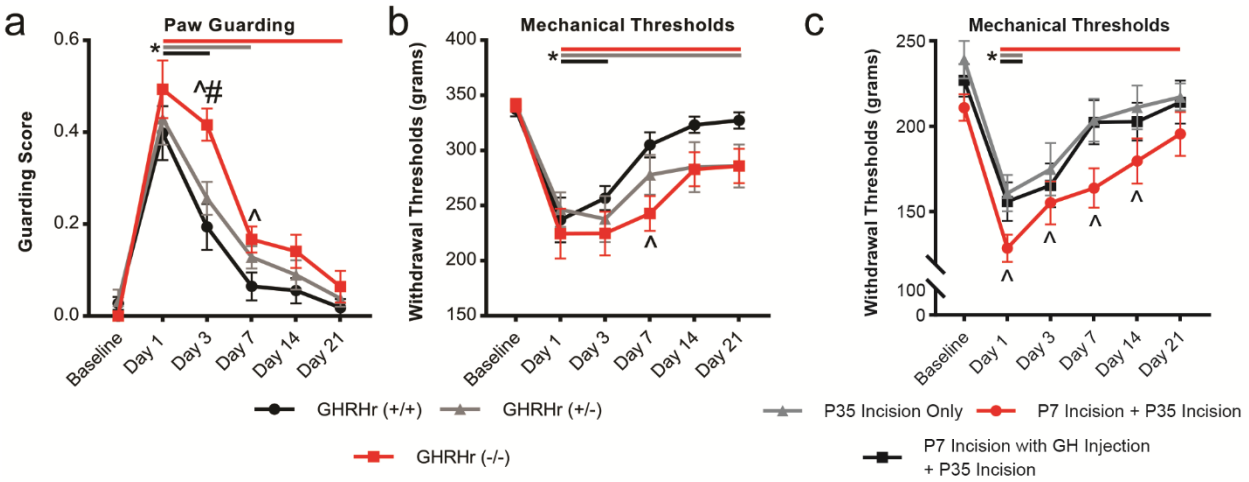
a
Paw Guarding
Guarding Score
0.6
0.4
0.2
0.0
*
^#
^
Baseline
Day 1
Day 3
Day 7
Day 14
Day 21
b
Mechanical Thresholds
Withdrawal Thresholds (grams)
400
350
300
250
200
150
*
^
c
Mechanical Thresholds
Withdrawal Thresholds (grams)
250
200
150
100
0
*
^
GHRHr (+/+)
GHRHr (+/-)
GHRHr (-/-)
P35 Incision Only
P7 Incision + P35 Incision
P7 Incision with GH Injection
+ P35 Incision

Figure 6.

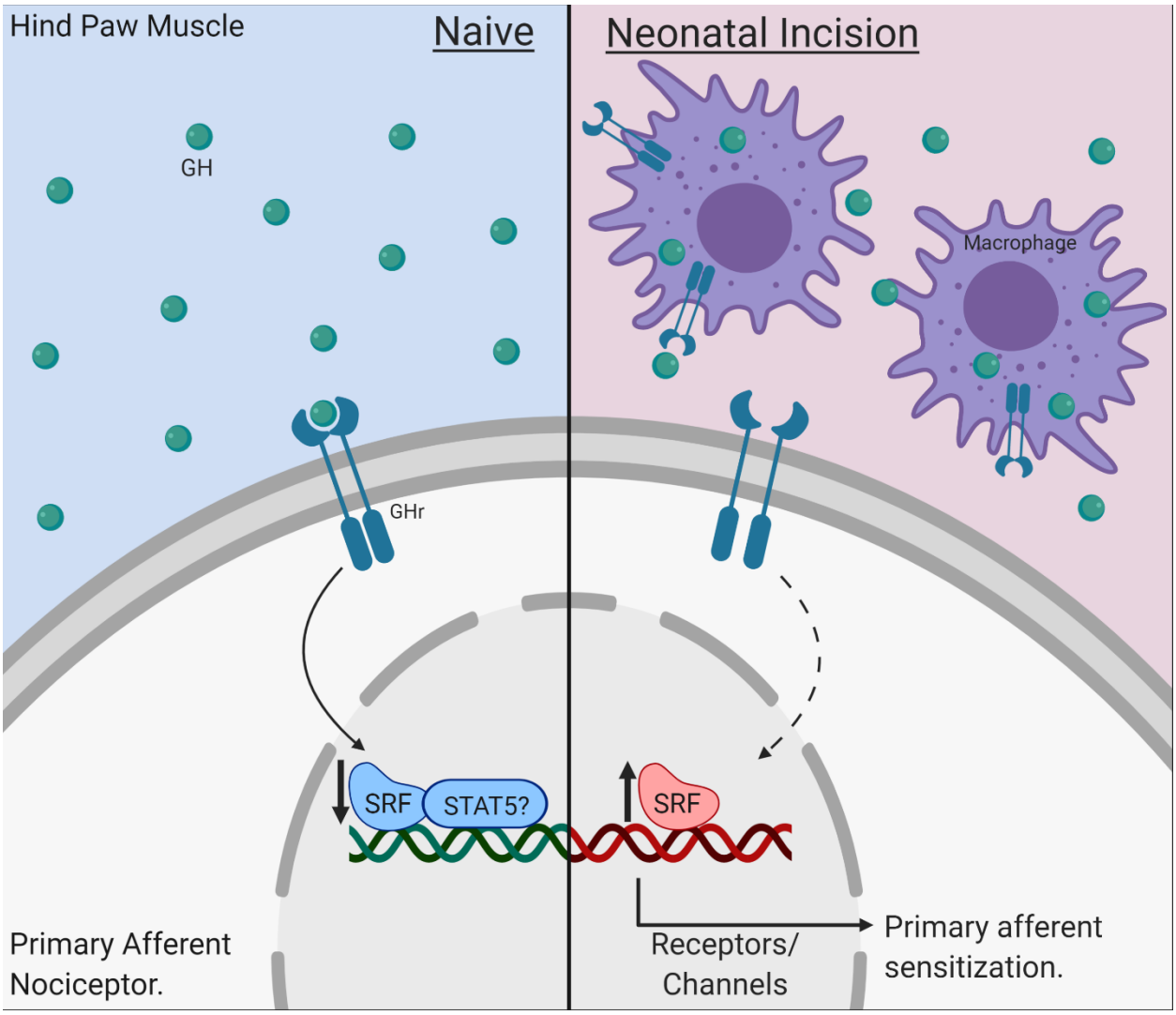
Hind Paw Muscle
Naive
Neonatal Incision
GH
Macrophage
GHr
SRF
STAT5?
SRF
Primary Afferent
Nociceptor.
Receptors/
Channels
Primary afferent
sensitization.

Table 1.

% Change in DRG mRNA

Gene	Incision + Vehicle	Incision + GH
IGFr1	258 ± 29%*	21 ± 14%
SRF	142 ± 19%*	27 ± 25%
TRPV1	178 ± 14%*	12 ± 15%
TRPA1	493 ± 41%*	1 ± 25%
STAT5	164 ± 20%*	69 ± 31%
P2X3	44 ± 22%*	-2 ± 18%
NFκB	83 ± 13%*	40 ± 11%
ASIC3	18 ± 10%	35 ± 11%
P2Y1	44 ± 15%	-14 ± 10%
ELK1	-29 ± 13%	-21 ± 15%
ELK3	-97 ± 5%*	-98 ± 15%*
ELK4	-28 ± 8%	-19 ± 9%
STAT1	92 ± 28%	10 ± 18%
STAT3	220 ± 7%*	164 ± 7%*
IL1-r	-50 ± 15%*	-51 ± 14%*
TNFa-r	15 ± 8%	13 ± 7%
GHr	15 ± 4%	16 ± 6%
Fcer2a	-81 ± 20%*	-80 ± 11%*
OSMr	-59 ± 17%*	-66 ± 16%*

% Change in Muscle mRNA

Gene	Incision + Vehicle	Incision + GH
MCP1	584 ± 24%*	276 ± 17%*
GDNF	204 ± 44%*	179 ± 23%*
IL1β	1098 ± 50%*	608 ± 40%*
NGF	77 ± 23%*	72 ± 20%*
TNFα	11 ± 20%	-40 ± 27%

Supplementary Information:

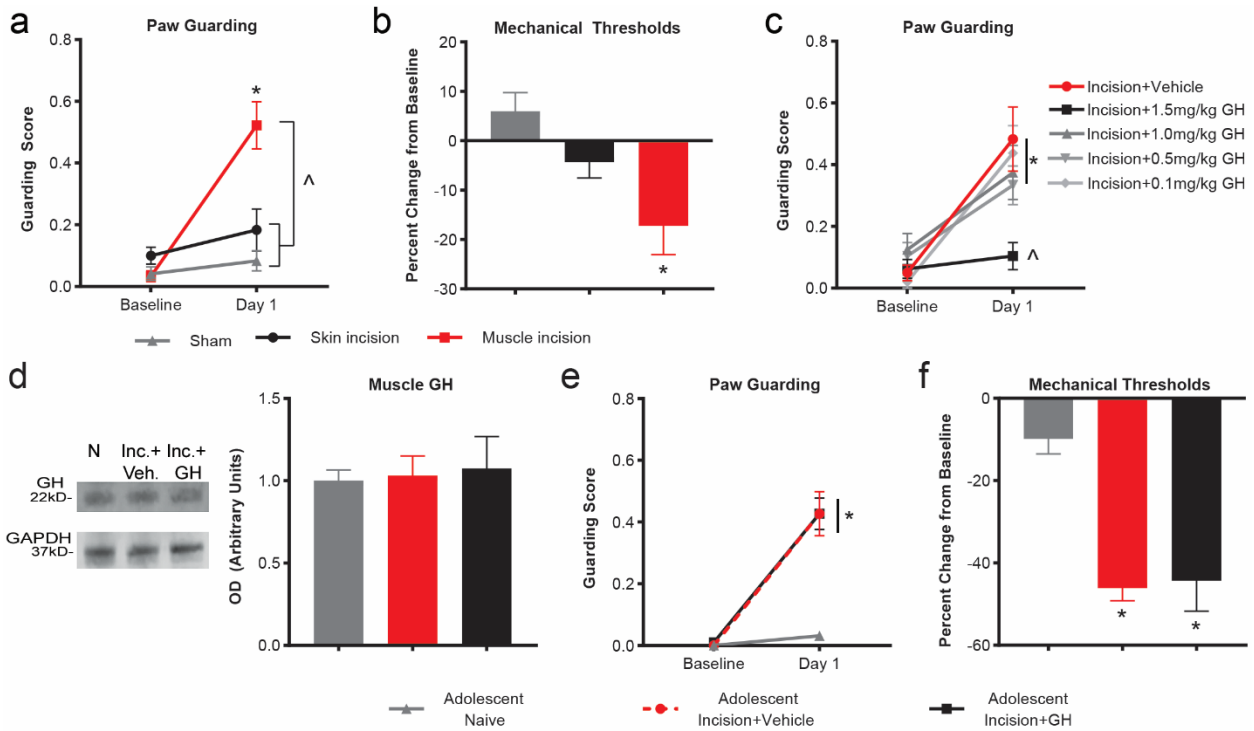

Supplementary Figure 1: Muscle incision produces measurable behavioral responses compared to controls. a, One day after a "reverse" neonatal muscle incision, animals guard the injured hindpaw compared to baseline and controls. Sham injured animals that received a suture through intact skin and dorsal skin incision only (not muscle) did not guard compared to baseline (BL). b, Only animals that received a muscle incision displayed lower squeezing withdrawal thresholds compared to BL. *p<0.001 vs. BL; ^p<0.001 vs. each control group. n = 10-15/group, two-way RM ANOVA, Tukey's post hoc. c, One day after an injury, animals dosed with GH at 0, 0.1, 0.5 and 1.0 mg/kg were significantly different from BL. Animals injected with 1.5 mg/kg did not differ from BL and had significantly lower guarding scores compared to vehicle injected animals at 1d. *p<0.05 vs. BL; ^p<0.001 vs. incision+vehicle. d, Representative images of western blots for GH in naïve, incised and GH treated incised animals. Quantification indicates no differences between groups. n = 4/group, one-way ANOVA. e, Adolescent animals with vehicle+incision or GH+incision guard one day after an injury compared to BL and naïve animals. f, After a hindpaw incision, both incised groups of P35 animals (vehicle and GH treated) display reduced mechanical withdrawal thresholds compared to BL and naïve. *p<0.001 vs. BL and naïve. n = 8/group, two-way RM ANOVA, Tukey's post hoc. Data shown as the mean ± s.e.m.

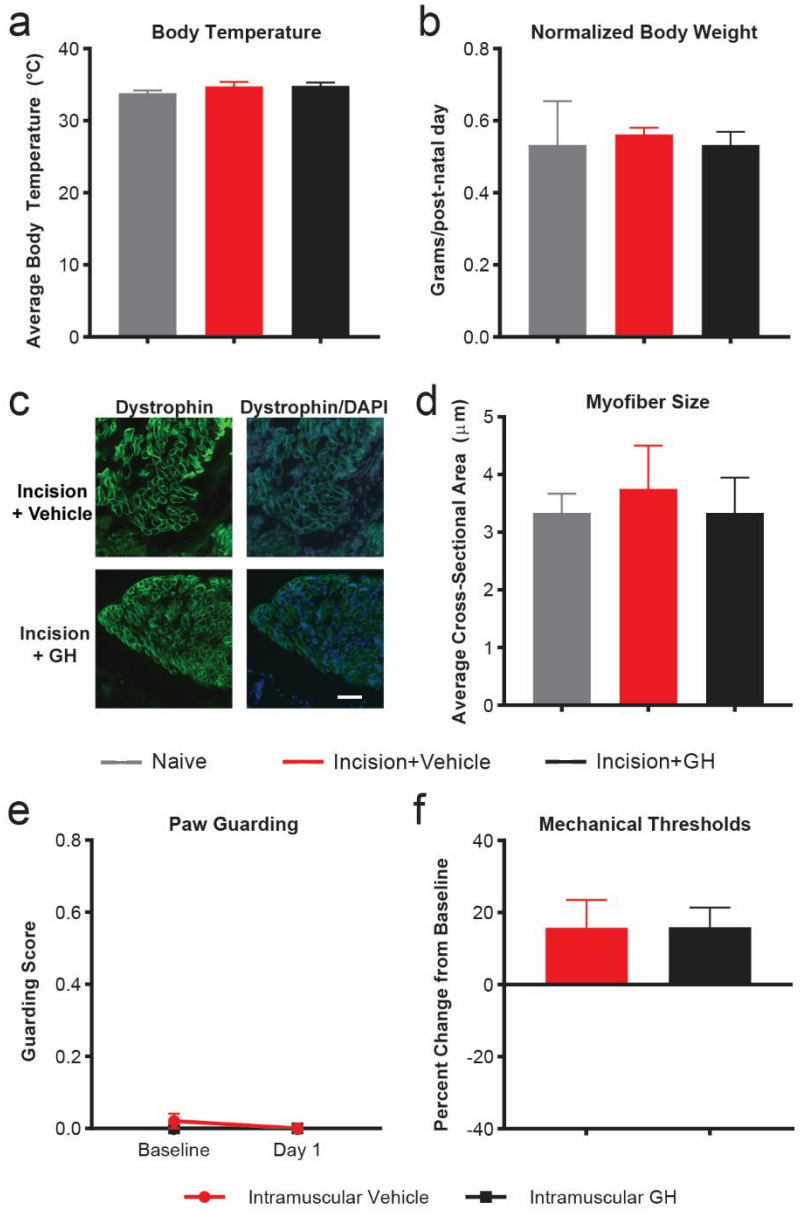

Supplementary Figure 2: Off-target analyses of local GH injections. a, Average body temperature measured on the thorax of neonates was not affected by injury or GH treatment. b, Body weight normalized to postnatal age was not affected by injury or GH injection. n = 4-6/group, one-way ANOVA. c, Representative images of myofibers stained with dystrophin (green) in both injured groups. DAPI (blue) co-stain was used to mark nuclei. d, The cross sectional area of injured animals was not affected by GH treatment. n = 3 animals/group, one-way ANOVA. e, Spontaneous paw guarding at Day 1 is not affected by local GH (1.5mg/kg) injection in mice without incision compared to baseline (BL). f, Evoked mechanical withdrawal thresholds are not affected by local GH injection alone. n = 7-8/group, one-way ANOVA.

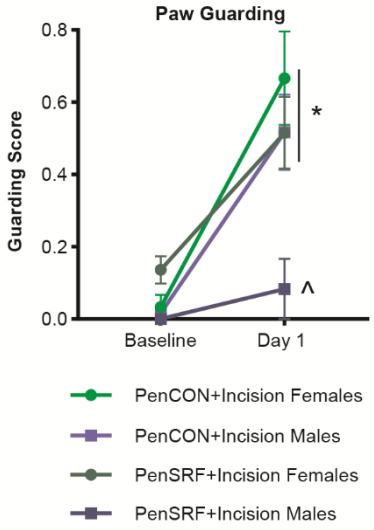

Supplementary Figure 3: Sex-related effects of SRF inhibition on paw guarding after incision. Neonates injected with PenCON prior to an injury display increased guarding 1d after an incision. Females injected with PenSRF also have significantly increased guarding at 1d. Males injected with PenSRF do not differ from BL and guard significantly less than females. *p<0.001 vs. BL; ^p<0.001 vs. females and other Day 1 conditions. PenCON males = 10, females = 5; PenSRF males = 5, females = 11. Three-way RM ANOVA (GraphPad v.8) (time x sex x condition), Tukey's post hoc. Data shown as the mean ± s.e.m.

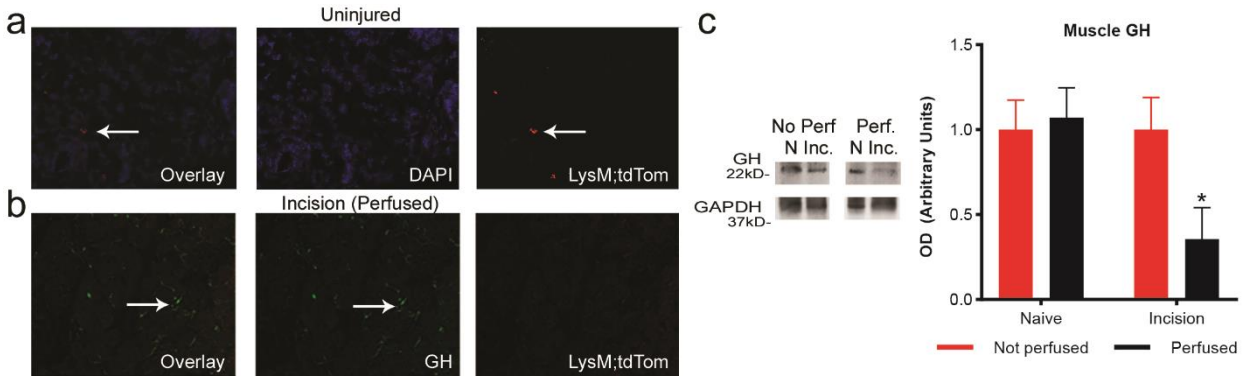

Supplementary Figure 4: Cardiac perfusion with ice-cold saline reduces macrophages and consequently GH levels after a neonatal incision. a, Representative images of uninjured hindpaw muscle from the macrophage reporter (LysM;tdTom) mouse co-stained with DAPI (blue) to mark nuclei. Arrows show few macrophages present in uninjured tissue. b, Images of injured hindpaw muscle in perfused LysM;tdTom animals (red) and stained for GH (green). Arrows indicate some remaining GH staining (compare to Figs. 4c, d). c, Representative western blots for GH in naïve and injured muscle with and without cardiac perfusion. Quantification of western blot analysis indicates that incised and perfused muscle have reduced GH levels compared to naïve unperfused. *$p<0.05$ vs. naïve unperfused. n = 4/group, two-way ANOVA, Tukey's post hoc. Data shown as the mean ± s.e.m.

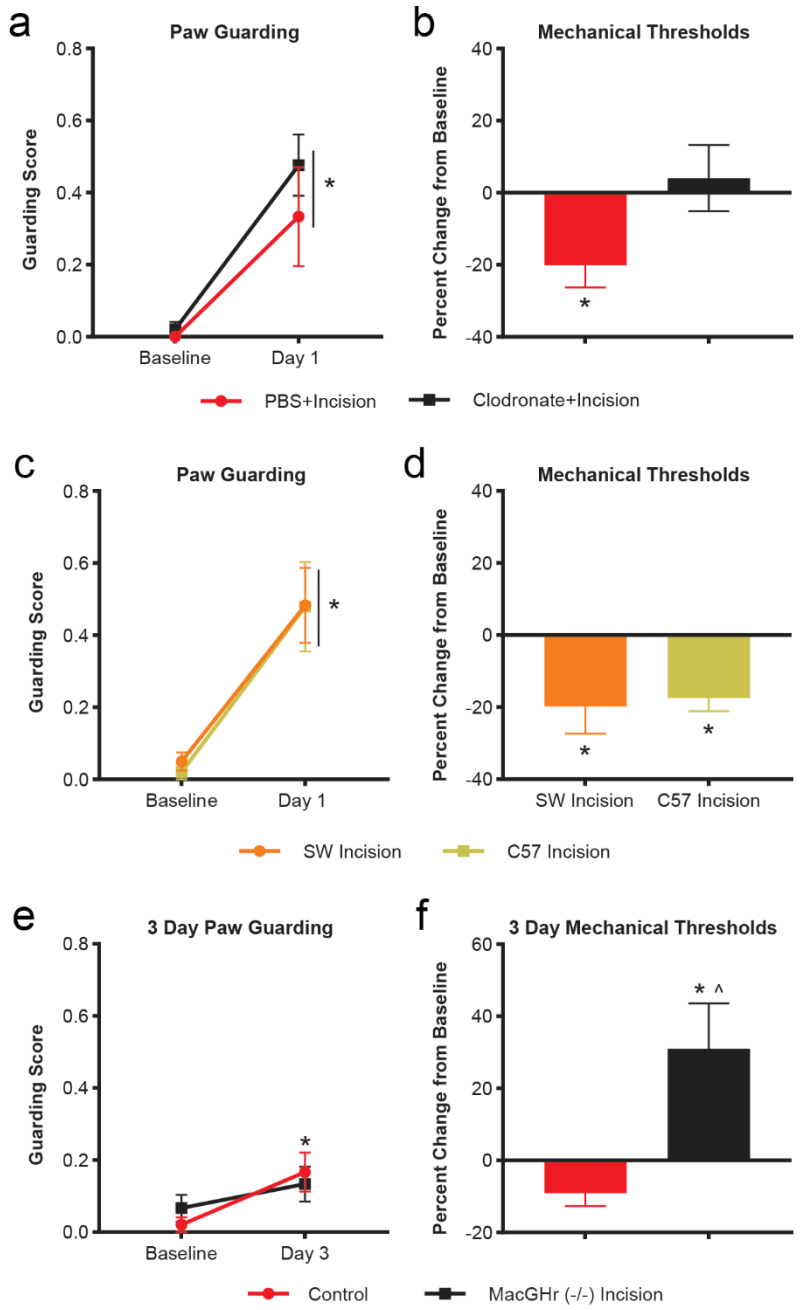

Supplementary Figure 5: Behavioral effects of depleting macrophages by liposome encapsulated clodronate in neonates with hindpaw incision. a, Animals guard after an injury regardless of intramuscular control PBS or clodronate injections. b, One day after an injury, PBS treated animals display reduced mechanical withdrawal thresholds, while clodronate treated animals do not. *p<0.05 vs. BL. n = 8/group, two-way RM ANOVA, Tukey's post hoc. c, One day after an injury, neonatal SW and C57 animals display spontaneous paw guarding compared to baseline values. d, Following an incision, neonatal animals from both strains display reduced squeezing withdrawal thresholds compared to baseline. *P<0.05 vs. BL. n = 8-10/group, two-way RM ANOVA, Tukey's post hoc. e, Three days after a neonatal incision MacGHr-/- animals no longer display a difference from baseline (BL), but C57 animals still slightly guard their paw. f, Mechanical withdrawal thresholds are increased in MacGHr-/- 3 days after a neonatal injury compared to their BL and controls. *p<0.05 vs. BL; ^p<0.05 vs. controls. n = 8-10/group, two-way RM ANOVA, Tukey's post hoc. Data shown as the mean ± s.e.m.

Group III/IV Instantaneous Frequencies									
Afferent Type	**Naïve**			**Incision + Vehicle**			**Incision + GH**		
(Hz)	**Mean**	**s.e.m.**	**n**	**Mean**	**s.e.m.**	**n**	**Mean**	**s.e.m.**	**n**
Mechanical	73	13	21	111	27	13	59	12	22
Cold	18.8	10.4	9.0	44.1	13.6	10.0	29.8	9.3	10.0
Hot	59.1	1.8	2.0	51.3	3.0	21.6	78.2	39.7	8.0
Low metabolite	24.7	22.3	4.0	4.5	n/a	1.0	192.9	104.7	3.0
High metabolite	14.8	7.3	5.0	18.9	11.1	4.0	27.1	2.8	2.0
Both metabolite	7.8	4.0	4.0	43.2	20.6	6.0	0.7	n/a	1.0

Group III/IV Thermal and Chemical Firing Rates									
Afferent Type	**Naïve**			**Incision + Vehicle**			**Incision + GH**		
(Hz)	**Mean**	**s.e.m.**	**n**	**Mean**	**s.e.m.**	**n**	**Mean**	**s.e.m.**	**n**
Cold	2.9	0.6	8.0	4.8	1.4	10.0	5.3	1.4	9.0
Hot	16.0	n/a	1.0	6.0	2.0	3.0	6.8	3.8	8.0
Low metabolite	2.4	0.9	7.0	2.1	0.5	7.0	2.8	1.0	5.0
High metabolite	3.4	0.1	7.0	5.8	3.0	9.0	1.0	n/a	1.0
Both metabolite	5.3	1.8	3.0	3.0	0.4	7.0	1.0	n/a	1.0

Supplementary Table 1: Group III/IV instantaneous frequencies are unaffected between conditions within afferent subtypes. One-way ANOVA with Tukey's or ANOVA on Ranks with Dunn's post hoc.

mRNA Primers		
Gene	**Forward**	**Reverse**
ASIC3	ATGAAACCTCCCTCAGGACTGG	AACTCCCCATAGTAGCGAACCC
ELK1	AAGAATTGGAAGCTGCAAGGGCTG	TGTTCTCTGTTAGGATGGCTGGGA
ELK3	ACACACACACAACCAAGATG	TCAGAGCGCTGGGATTATAG
ELK4	GGTGATTTGTCGGAGAGTAG	CACCTCCTATCTCTGGGTAT
Fcer2a	GATCTAAGGAACGCCCAATC	CTGTGCGCTTCTCATTCA
GAPDH	ATGTGTCCGTCGTGGATCTGA	ATGCCTGCTTCACCACCTTCTT
GDNF	AGCTGCCAGCCCAGAGAATT	GCACCCCCGATTTTTGC
GHr	GCCTCTACACCGATGAGTAA	GGAAAGGACTACACCACCT
IGFr1	TTGAACTTATGCGCATGTGCTGGC	TCTCATCCTTGATGCTGCCGATGA
IL1-r	AGGAATGTGGCTGAAGAGCACAGA	ACTCGTGTGACCGGATATTGCTTC
IL1β	TACAAGGAGAACCAAGCAAC	GGTGTGCCGTCTTTCATTA
MCP1	CACCTGCTGCTACTCATTC	CTACAGCTTCTTTGGGACAC
NFκB	CTGCACCAAGACGGAACC	GAGCCTTCTCAAGAAAGAGGTTATC
NGF	ACACTCTGATCACTGCGTTTTTG	CCTTCTGGGACATTGCTATCTGT
OSMr	TCCAGGCTCACCCTTATT	AGCCTCGGTGTGTAGTT
P2X3	ACAAGATGGAGAATGGCAGCGAGT	TGATGTTGAACTTGCCAGCGTTCC
P2Y1	GATGAATTTGCGAGCACGGTTGGA	TCCACACAGCTGTTGAGACTTGCT
SRF	TGGAGTTCATCGACAACAAG	AGCGTGGACAGCTCATA
STAT1	CCCAGGAATCTCTCCTTCTT	GACCTCTCTTGGTGACTGAT
STAT3	CTGGGTCTGGCTAGACAATA	CGCTCCTTGCTGATGAAA
STAT5	CCCACGTCAGTTGTAGTATC	GTTCAGCTCTTACACGAGAG
TNFa-r	TCGGAAAGAAATGTCCCAGGTGGA	TGGAACTGGTTCTCCTTACAGCCA
TNFα	CCTATGTCTCAGCCTCTTCT	GGGAACTTCTCATCCCTTTG
TRPA1	GCAGGTGGAACTTCATACCAACT	CACTTTGCGTAAGTACCAGAGTGG
TRPV1	TTCCTGCAGAAGAGCAAGAAGC	CCCATTGTGCAGATTGAGCAT

Supplementary Table 2: Primer information for standard PCR.